

Measurements of the ρ and η parameters of the V_{CKM} matrix and perspectives.

P. Paganini* , F. Parodi+ , P. Roudeau and A. Stocchi

Laboratoire de l'Accélérateur Linéaire
IN2P3-CNRS et Université de Paris-Sud

Abstract

A review of the current status of the Cabibbo-Kobayashi-Maskawa matrix (V_{CKM}) is presented and a special emphasis is put on the determination of the ρ and η parameters. From this study it follows that, in the Standard Model, the $B_s^0\text{-}\overline{B}_s^0$ oscillation frequency, Δm_s , has to lie, with 68% C.L., between 6.5 ps^{-1} and 15 ps^{-1} , and is below 21 ps^{-1} at 95% C.L.. If the interest of measuring Δm_s is underlined, the importance of a precise determination of the B meson decay constant, f_B , is also stressed. It is proposed to obtain a precise value for this parameter from an accurate measurement of f_D , the D meson decay constant, using results from lattice QCD to relate D and B hadrons. A future Tau-Charm factory could accomplish this task. It is also shown that from the present measurements, assuming the validity of the Standard Model, an already accurate value of $\sin 2\beta = 0.67_{-0.13}^{+0.12}$ is obtained. So far no constraint can be obtained on $\sin 2\alpha$. The interest of having a direct measurement of $\sin 2\alpha$ and $\sin 2\beta$ at B-factories or at other facilities is reminded. Finally constraints on SUSY parameters, in the framework of a given model, obtained from a precise measurement of the CKM matrix elements are analyzed.

To be submitted to Physica Scripta

(DELPHI 97-137 PHYS 724 and LAL-97-79)

* Now at École Polytechnique, LPNHE, Palaiseau
+ on leave of absence of the INFN-Genova

1 Introduction

The search for CP violation in B meson decays, at B-factories or high energy hadron colliders, is usually justified by the quest to explain the asymmetry matter-antimatter in the Universe [1]. The Standard Model CP violation, which is contained in the Cabibbo, Kobayashi, Maskawa matrix, fails by about 10 orders of magnitude to account for the measured abundance of baryons [2]. It is then necessary to invoke non-Standard Model sources of CP violation and many possibilities exist. As an example, in the Supersymmetric extension of the Standard Model, additional phases are present but there is no guarantee that these phases produce measurable effects in B decays or that they can really account for the cosmological excess of baryons.

In this paper, a pragmatic attitude has been adopted which consists in considering the limiting factors on the precision of consistency tests of the Standard Model predictions and a special emphasis has been placed on the control of uncertainties coming from the strong interaction operating in the non-perturbative regime.

In the Standard Model, weak interactions among quarks are codified in a 3×3 unitary matrix: the V_{CKM} matrix. The existence of this matrix conveys the fact that quarks which participate to weak processes are a linear combination of mass eigenstates. The V_{CKM} matrix can be parametrized in terms of four parameters: λ , A , ρ and η and the Standard Model predicts relations between the different processes which depend on these parameters; CP violation is one of those. The unitarity of the V_{CKM} matrix can be visualized as a triangle in the $\rho - \eta$ plane. Several quantities which depend on ρ and η can be measured and, if the Standard Model is correct, they must define compatible values for the two parameters, inside measurement errors and theoretical uncertainties. Extensions of the Standard Model, as Supersymmetry, provide different parametrizations, for the same observables, and additional parameters to ρ and η . The position of the summit of the unitarity triangle, given by the ρ and η coordinates, will be different in this scenario. It has to be stressed that only the extensions of the Standard Model in which the flavour changes are controlled by the V_{CKM} matrix are considered in this paper.

It is thus of interest to measure accurately as many observables as possible to have evidence for physics outside the Standard Model. By the year 2000, HERA-B and B-factories are expected to measure CP violation phases which are directly related to the angles α and β of the unitarity triangle. The aim of this paper is to review present constraints on ρ and η obtained from existing measurements of $B_{d,s}^0 - \overline{B}_{d,s}^0$ oscillations, CP violation in the K system and $b \rightarrow u\ell\overline{\nu}_\ell$ transitions. With the same constraints, and considering the expected improvements of current analyses and of lattice QCD evaluations, possible uncertainties on ρ and η have been evaluated from future measurements. After the year 2000, the contribution from precise measurements at a Tau-Charm factory, has been also considered. It is shown that a well defined region, in the (ρ, η) plane, can be obtained, independently of the measurements of the angles α and β of the unitarity triangle. As these angles are expected to be measured at the same time, with a reasonable accuracy, it will be of interest to verify if the two approaches give compatible results.

2 The Cabibbo-Kobayashi-Maskawa (CKM) matrix : an historical introduction

In the early 60's there were three quark flavours. The quark u with charge $+2/3$, the quarks d and s of charge $-1/3$. By analogy with leptons it was suggested that the quarks were also organized into doublets and the existence of a new quark of charge $2/3$ was proposed [3]. An intense experimental activity on strange particles shown, at the same time, that the absolute decay rate for $\Delta S = 1$ transitions was suppressed by a factor of about 20 as compared to $\Delta S = 0$ transitions.

In 1963 Cabibbo proposed [4] a model to account for this effect. In this model the d and s quarks, involved in weak processes, are rotated by a mixing angle θ_c : the Cabibbo angle. The quarks are organized in a doublet :

$$\begin{pmatrix} u \\ d_c \end{pmatrix} = \begin{pmatrix} u \\ d \cos\theta_c + s \sin\theta_c \end{pmatrix} \quad (1)$$

the small value of θ_c ($\simeq 0.22$) is responsible for the suppression of strange particle decays (the coupling being proportional to $\sin^2\theta_c$). In this picture the slight suppression of $n \rightarrow pe^- \bar{\nu}_e$ with respect to the rate of $\mu^- \rightarrow e^- \nu_\mu \bar{\nu}_e$ is also explained by the fact that the coupling in the neutron decay is proportional to $\cos^2\theta_c$.

In the other hand, in this model, the neutral current coupling is of the form

$$u\bar{u} + d\bar{d}\cos^2\theta_c + s\bar{s}\sin^2\theta_c + (s\bar{d} + d\bar{s})\cos\theta_c\sin\theta_c. \quad (2)$$

The presence of the $(s\bar{d} + d\bar{s})$ term implies the existence of a flavour changing neutral current (FCNC). This was a serious problem for the Cabibbo model, since all the observed neutral current processes were characterized by the selection rule $\Delta S = 0$.

In 1970 Glashow, Iliopoulos and Maiani [5] (GIM) proposed the introduction of a new quark, named c , of charge $2/3$ and the introduction of a new doublet of quarks formed by the c quark and by a combination of the s and d quarks orthogonal to d_c :

$$\begin{pmatrix} c \\ s_c \end{pmatrix} = \begin{pmatrix} c \\ s \cos\theta_c - d \sin\theta_c \end{pmatrix}. \quad (3)$$

In this way the $(s\bar{d} + d\bar{s})$ term in the neutral current disappears.

The discovery of the charm quark in the form of $c\bar{c}$ bound states [6] and the observation of charmed particles decaying into strange particles [7] (the $c\bar{s}$ transitions which are proportional to $\cos^2\theta_c$ dominate over the $c\bar{d}$ transitions which are proportional to $\sin^2\theta_c$) represent a tremendous triumph of this picture.

The charge current can then be written:

$$(\bar{u}c)\gamma^\mu(1 - \gamma_5)V \begin{pmatrix} d \\ s \end{pmatrix} \quad (4)$$

where u, d, s, c are the mass eigenstates and V is defined as:

$$V = \begin{pmatrix} \cos\theta_c & \sin\theta_c \\ -\sin\theta_c & \cos\theta_c \end{pmatrix}. \quad (5)$$

V is the Cabibbo unitary matrix which specifies the quark states which are involved in weak interactions. This matrix express the fact that there is an arbitrary rotation, usually

applied to the $-1/3$ charged quarks, which is due to the mismatch between the strong and the weak eigenstates.

In 1975 the Mark I group at SPEAR discovered the third charged lepton : the τ [8]. Two years later the fifth quark, the b , was also found at FNAL [9]. The indirect existence for the top quark t from the observation of $B_d^0 - \overline{B}_d^0$ oscillations [10] suggested the existence of a heavier version of the doublets (u,d) and (c,s) (the t quark has been recently discovered at Fermilab [11] in $p\overline{p}$ collisions)

The existence of three quark doublets was already proposed by Kobayashi and Maskawa in 1973 [12] as a possible explanation of CP violation. Their proposal is a generalization of the Cabibbo rotation and implies that the weak flavour changing transitions are described by a 3×3 unitary matrix:

$$\begin{pmatrix} u \\ c \\ t \end{pmatrix} \rightarrow V \begin{pmatrix} d \\ s \\ b \end{pmatrix}, \quad V = \begin{pmatrix} V_{ud} & V_{us} & V_{ub} \\ V_{cd} & V_{cs} & V_{cb} \\ V_{td} & V_{ts} & V_{tb} \end{pmatrix}. \quad (6)$$

This matrix can be parametrized using three real parameters and one phase which cannot be removed by redefining the quark field phases. This phase leads to the violation of the CP symmetry. In fact since CPT is a good symmetry for all quantum field theories, the complexity of the Hamiltonian implies that the time reversal invariance T and thus CP is violated. In this picture the Standard Model includes CP violation in a simple way.

Several parametrizations of the V_{CKM} matrix exist.

The standard parametrization is [13] :

$$V_{CKM} = \begin{pmatrix} c_{12}c_{13} & s_{12}c_{13} & s_{13}e^{-i\delta_{13}} \\ -s_{12}c_{23} - c_{12}s_{23}s_{13}e^{i\delta_{13}} & c_{12}c_{23} - s_{12}s_{23}s_{13}e^{i\delta_{13}} & s_{23}c_{13} \\ s_{12}s_{23} - c_{12}c_{23}s_{13}e^{i\delta_{13}} & -c_{12}s_{23} - s_{12}c_{23}s_{13}e^{i\delta_{13}} & c_{23}c_{13} \end{pmatrix} \quad (7)$$

where c_{ij} and s_{ij} stand for $\cos\theta_{ij}$ and $\sin\theta_{ij}$ respectively, the indices 1, 2, 3 represent the generation label and δ_{13} is the phase. Experimentally there is a hierarchy in the magnitude of these elements. The parametrization proposed by Wolfenstein [14], in terms of four parameters: λ , A , ρ and η , is motivated by this observation. By definition these parameters verify the following expressions:

$$s_{12} = \lambda, \quad s_{23} = A\lambda^2, \quad s_{13}e^{-i\delta_{13}} = A\lambda^3(\rho - i\eta).$$

The V_{CKM} matrix elements can be expanded in powers of λ and, without any prejudice on the possible values for A , ρ and η , expressions valid up to $O(\lambda^6)$ have been obtained :

$$V_{CKM} = \begin{pmatrix} 1 - \frac{\lambda^2}{2} - \frac{\lambda^4}{8} & \lambda & A\lambda^3(\rho - i\eta) \\ -\lambda + \frac{A^2\lambda^5}{2}(1 - 2\rho) - iA^2\lambda^5\eta & 1 - \frac{\lambda^2}{2} - \lambda^4(\frac{1}{8} + \frac{A^2}{2}) & A\lambda^2 \\ A\lambda^3(1 - (1 - \frac{\lambda^2}{2})(\rho + i\eta)) & -A\lambda^2(1 - \frac{\lambda^2}{2})(1 + \lambda^2(\rho + i\eta)) & 1 - \frac{A^2\lambda^4}{2} \end{pmatrix} \quad (8)$$

η accounts for the CP violating phase. This parametrization is still approximated but is completely adequate to the arguments developed in this paper.

This parametrization shows that the matrix is almost diagonal, namely that the coupling between quarks of the same family is close to unity, and is decreasing as the separation between families increases.

3 The A and λ parameters

The λ parameter has been measured using strange particle decays involving the $s \rightarrow u$ transitions. It is obtained from the measurement of K_{l3} decays : $K^+ \rightarrow \pi^0 \ell^+ \nu_e$ or $K_L^0 \rightarrow \pi^- \ell^+ \nu_e$ and from hyperons semileptonic decays. The average of these measurements is [13]:

$$|V_{us}| = \lambda = 0.2205 \pm 0.0018 \quad (9)$$

Studies of $c \rightarrow d$ transitions, in neutrino production of charmed particles and in charmed particle decays into non-strange states, give a compatible determination of λ which is nearly ten times less precise [13]

$$|V_{us}| = \lambda = 0.224 \pm 0.016 \quad (10)$$

The average of the previous determinations gives the following value for λ :

$$\lambda = 0.2205 \pm 0.0018 \quad (11)$$

In the Wolfenstein parametrization the parameter A is introduced and defined from the expression :

$$|V_{cb}| = A\lambda^2 \quad (12)$$

The value of $|V_{cb}|$ can be determined in two ways :

- from LEP measurements of the inclusive lifetime, τ_b , and of the semileptonic branching fraction (BR_{sl}^b) of B hadrons. $|V_{cb}|$ can be obtained from the following expression :

$$|V_{cb}|^2 = \frac{BR_{sl}^b}{\gamma_c \tau_b}. \quad (13)$$

The term γ_c includes the dependence on m_b, m_c and contains also QCD corrections. An analogous definition is valid at the $\Upsilon(4S)$ using the measured branching ratio, $Br(B \rightarrow \ell^+ \nu X)$, and the average B^+/B_d^0 lifetimes. The use of experimental data and of theoretical models [15] is subject to an intense discussion [16]. A detailed review can be found in [17] [18] [19]. From the values given in Table 1 and using the relation (13), $|V_{cb}|$ has been evaluated to be:

$$|V_{cb}| = 0.0405 \pm 0.0005 \pm 0.0030. \quad (14)$$

The second quoted error reflects theoretical uncertainties on the parameter γ_c and it has been overestimated according to the authors of [20].

- from the interpretation of the measurement of the exclusive branching fraction, $BR(B \rightarrow D^* \ell \nu)$, in the HQET framework [23]. The measurements done at the $\Upsilon(4S)$ and at LEP [24] give:

$$F(1) |V_{cb}| = 0.0357 \pm 0.0021 \pm 0.0014. \quad (15)$$

Using for $F(1)$, which deviates from unity because of strong interactions, the value [23]:

$$F(1) = 0.91 \pm 0.03 \quad (16)$$

it follows:

$$|V_{cb}| = 0.0392 \pm 0.0027 \pm 0.0013. \quad (17)$$

Variables	results	references
τ_b	$1.566 \pm 0.017 \text{ ps}$	[21]
$\tau_{B_d^0}$	$1.55 \pm 0.04 \text{ ps}$	[21]
τ_{B^+}	$1.66 \pm 0.04 \text{ ps}$	[21]
$Br(b \rightarrow \ell^+ \nu X)(LEP)$	$11.22 \pm 0.21\%$	[22]
$Br(B \rightarrow \ell^+ \nu X)(\Upsilon(4S))$	$10.43 \pm 0.24\%$	[13]
γ_c	$41 \pm 6 \text{ ps}^{-1}$	[16]

Table 1: *Theoretical and experimental inputs used in the evaluation of V_{cb} .*

Assuming that the theoretical uncertainties are uncorrelated and averaging the two previous determinations, $|V_{cb}|$ results to be :

$$|V_{cb}| = 0.0397 \pm 0.0020 \quad (18)$$

which corresponds to:

$$A = 0.81 \pm 0.04 \quad (19)$$

4 The unitarity triangle

From the unitarity of the CKM matrix ($VV^\dagger = 1$) three independent equations relating its elements can be written. In particular, in transitions involving b quarks, the scalar product of the third column with the complex conjugate of the first row must vanish :

$$V_{ud}^* V_{ub} + V_{cd}^* V_{cb} + V_{td}^* V_{tb} = 0 \quad (20)$$

Using the parametrization given in eq. (8), and neglecting contributions of order $O(\lambda^7)$, the different terms, in this expression, are respectively:

$$V_{ud}^* V_{ub} = A\lambda^3(\bar{\rho} - i\bar{\eta}), \quad V_{cd}^* V_{cb} = -A\lambda^3, \quad V_{td}^* V_{tb} = A\lambda^3(1 - \bar{\rho} + i\bar{\eta}) \quad (21)$$

where the parameters $\bar{\rho}$ and $\bar{\eta}$ have been introduced [25]:

$$\bar{\rho} = \rho(1 - \frac{\lambda^2}{2}) \quad ; \quad \bar{\eta} = \eta(1 - \frac{\lambda^2}{2}).$$

The three expressions are proportional to $A\lambda^3$ which can be factored out and the geometrical representation of eq. (20), in the $(\bar{\rho}-\bar{\eta})$ plane, is a triangle with summits at C(0,0), B(1,0) and A($\bar{\rho}-\bar{\eta}$) (see Figure 1) The following relations hold :

$$\begin{aligned} \overline{AC} &= \frac{1 - \frac{\lambda^2}{2}}{\lambda} \frac{|V_{ub}|}{|V_{cb}|} = \sqrt{(\bar{\rho}^2 + \bar{\eta}^2)} \\ \overline{AB} &= \frac{|V_{td}|}{\lambda |V_{cb}|} = \sqrt{((1 - \bar{\rho})^2 + \bar{\eta}^2)} \\ \overline{AB} &= \frac{1 - \frac{\lambda^2}{2}}{\lambda} \frac{|V_{td}|}{|V_{ts}|} = \sqrt{((1 - \bar{\rho})^2 + \bar{\eta}^2)} \end{aligned} \quad (22)$$

these expressions are valid up to $O(\lambda^4)$.

The Standard Model, with three families of quarks and leptons, predicts that all measurements have to be consistent with the point A($\bar{\rho} - \bar{\eta}$).

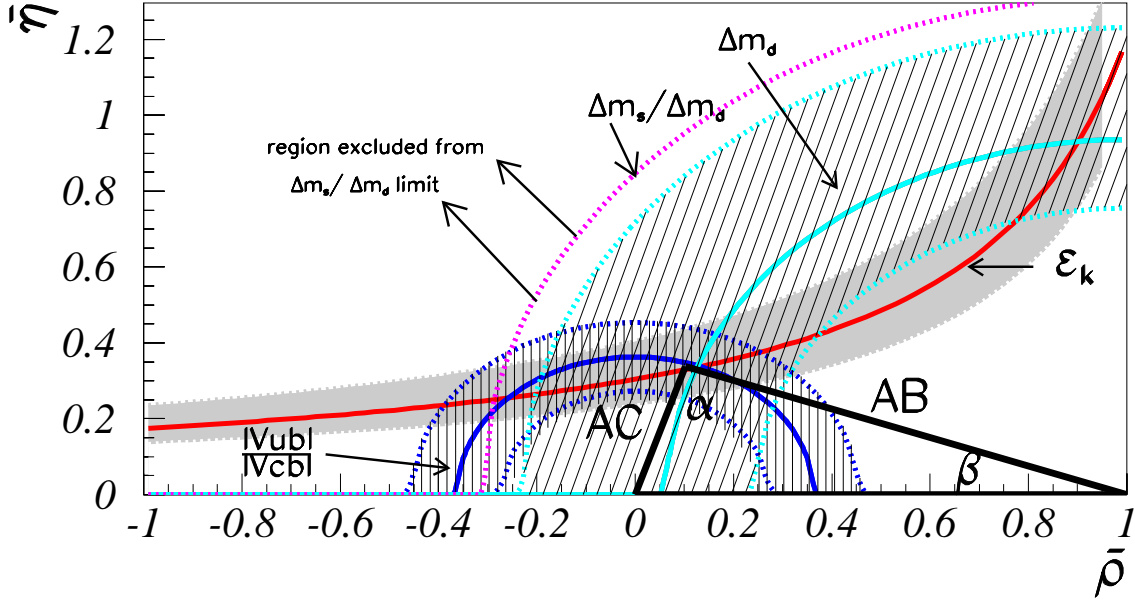


Figure 1: The unitarity triangle in the $(\bar{\rho}-\bar{\eta})$ plane. The constraints on Δm_d , $|\epsilon_K|$ and $\frac{|V_{ub}|}{|V_{cb}|}$ are shown as bands corresponding to $\pm 1\sigma$. The 95 % C.L. excluded region obtained from the limit on the ratio $\Delta m_s/\Delta m_d$ corresponds to the area situated on the left of the line.

4.1 Charmless semileptonic decays of B mesons.

The presence of leptons above the kinematical limit for leptons produced in the decay $B \rightarrow D\ell\bar{\nu}_\ell$, at the $\Upsilon(4S)$, is attributed to $b \rightarrow u\ell\bar{\nu}_\ell$ transitions. As only a small fraction of the energy spectrum of these leptons is accessible experimentally, there is, at present, a large systematic uncertainty in the modelling of these transitions to evaluate the value of $|V_{ub}|$ [13]:

$$\frac{|V_{ub}|}{|V_{cb}|} = 0.08 \pm 0.02. \quad (23)$$

This measurement corresponds to the following constraint in the $(\bar{\rho}-\bar{\eta})$ plane:

$$\sqrt{\bar{\rho}^2 + \bar{\eta}^2} = 0.35 \pm 0.09. \quad (24)$$

4.2 CP violation in the $K^0 - \bar{K}^0$ system.

Indirect CP violation in the $K^0 - \bar{K}^0$ system is usually expressed in terms of the $|\epsilon_K|$ parameter which is the fraction of the CP violating component in the mass eigenstates. Replacing $|V_{cs}|$ by its expression in terms of the Wolfenstein parameters, the following equation is obtained, having neglected $O(\lambda^4)$ terms:

$$|\epsilon_K| = C_\epsilon B_K A^2 \lambda^6 \bar{\eta} \left[-\eta_1 \left(1 - \frac{\lambda^2}{2} \right) S(x_c) + A^2 \lambda^4 (1 - \bar{\rho} - (\bar{\rho}^2 + \bar{\eta}^2) \lambda^2) \eta_2 S(x_t) + \eta_3 S(x_c, x_t) \right]. \quad (25)$$

Another contribution, proportional to the ratio $\xi = Im(A(K \rightarrow \pi\pi)_{I=0})/Re(A(K \rightarrow \pi\pi)_{I=0})$, which is at most a 2% correction to ϵ_K [26] has been also neglected. The constant $C_\epsilon = \frac{G_F^2 f_K^2 m_K m_W^2}{6\sqrt{2}\pi^2 \Delta m_K}$ is equal to 3.85×10^4 (see Table 2). The η_i parameters include perturbative QCD corrections which have been evaluated recently at the next to leading order [27] [28]:

$$\eta_1 = 1.38 \pm 0.53, \quad \eta_2 = 0.574 \pm 0.004, \quad \eta_3 = 0.47 \pm 0.04. \quad (26)$$

The expressions for $S(x_c)$ and $S(x_c, x_t)$ depend on $x_q = \frac{m_q^2}{m_W^2}$. An important theoretical uncertainty in eq. (25) comes from the “bag” parameter B_K which is of non-perturbative QCD origin. From recent lattice QCD evaluations the following value can be quoted [29]:

$$B_K(2GeV) = 0.66 \pm 0.02 \pm 0.06. \quad (27)$$

The first error corresponds to the present uncertainty of this evaluation inside the quenched approximation and the second error is related to the quenched approximation itself. The scale-invariant value for B_K is then evaluated, so that it will be consistent with the conventions used to obtain the η_i parameters [28]:

$$B_K = (\alpha_s^{(3)}(\mu))^{-\frac{2}{9}} (1 + \frac{\alpha_s^{(3)}(\mu)}{4\pi} J_3) B_K(\mu). \quad (28)$$

In this expression, $J_3 = \frac{307}{162}$, $\Lambda_{QCD}^{(3)} = 371 \text{ MeV}$ and the following value is obtained for B_K using $\mu = 2 \text{ GeV}$:

$$B_K = 0.90 \pm 0.09. \quad (29)$$

4.3 $B_d^0 - \overline{B}_d^0$ oscillations.

In the Standard model, the mass difference between the mass eigenstates in the $B_d^0 - \overline{B}_d^0$ system can be expressed as:

$$\Delta m_d = \frac{g^4}{192 m_W^2 \pi^2} |V_{tb}|^2 |V_{td}|^2 m_{B_d} f_{B_d}^2 B_{B_d} \eta_B x_t F(x_t), \quad (30)$$

where $g^2 = \frac{G_F}{\sqrt{2}} 8 m_W^2$. In this expression only terms in which the top quark contributes have been retained because they dominate. The mixed term with top and charm quark is almost 600 times smaller than the dominant one; the one involving only charm quarks is suppressed by an extra factor ten [30]. The function $F(x_t)$ is given by:

$$F(x_t) = \frac{1}{4} + \frac{9}{4} \frac{1}{(1-x_t)} - \frac{3}{2} \frac{1}{(1-x_t)^2} - \frac{3}{2} \frac{x_t^2}{(1-x_t)^3} \ln x_t \quad (31)$$

where $x_t = (m_t^2/m_W^2)$. $F(x_t)$ has a smooth variation with x_t and is equal to 0.54, for $m_t = 180 \text{ GeV}/c^2$. The scale for the evaluation of perturbative QCD corrections entering into η_B and the running of the t quark mass have to be defined in a consistent way [28]. The measured value of the pole top quark mass obtained by CDF and D0 collaborations ($m_t^{\text{pole}} = 175 \pm 6 \text{ GeV}/c^2$ [11]) has to be corrected downwards by $(7 \pm 1) \text{ GeV}/c^2$. The following values have been used:

$$m_t = 168 \pm 6 \text{ GeV}/c^2, \quad \eta_B = 0.55 \pm 0.01. \quad (32)$$

The dominant uncertainties in eq. (30) comes from the evaluation of the B meson decay constant f_{B_d} and of the “bag” parameter B_{B_d} . There is a vast literature on lattice QCD calculations of f_B . From the reviews [31] based on recent studies [32], the preferred value is :

$$f_{B_d} = 175 \pm 25 \pm 30 \text{ MeV} \quad (33)$$

where the first uncertainty is obtained using the quenched approximation and the second uncertainty accounts for the use of this approximation itself. These results are compatible with those obtained using sum rules technique [33], the relativistic quark model [34] and the QCD potential model [35].

The bag factor B_{B_d} has been evaluated using lattice QCD in a way which is consistent with the result quoted for B_K . At the 2 GeV scale, the following value from lattice QCD is obtained:

$$B_{B_d}(2 \text{ GeV}) = 0.95 \pm 0.07 \pm 0.09, \quad (34)$$

where the errors have the same meaning as in eq. (33). The scale-invariant value for B_{B_d} has been obtained using the following expression [27]:

$$B_{B_d} = (\alpha_s^{(5)}(\mu))^{-\frac{6}{23}} (1 + \frac{\alpha_s^{(5)}(\mu)}{4\pi} J_5) B_{B_d}(\mu), \quad (35)$$

in which $J_5 = \frac{5165}{3174}$ and gives:

$$B_{B_d} = 1.36 \pm 0.16. \quad (36)$$

Due to the dependence in $f_{B_d}^2 \times B_{B_d}$ in the expression of Δm_d (eq. 30), the uncertainty on f_{B_d} dominates over the one on B_{B_d} . The variable $f_{B_d} \sqrt{B_{B_d}}$ will be used often in the following and from expressions (33) and (36) its value is equal to:

$$f_{B_d} \sqrt{B_{B_d}} = 200 \pm 50 \text{ MeV} \quad (37)$$

The relative uncertainty on the square of this variable, which enters into expression (30), is then at the level of 50%. Using the parametrization given in eq. (30) the expression for Δm_d becomes:

$$\Delta m_d = \frac{g^4}{192 m_W^2 \pi^2} A^2 \lambda^6 [(1 - \bar{\rho})^2 + \bar{\eta}^2] m_{B_d} f_{B_d}^2 B_{B_d} \eta_{B_d} F(x_t). \quad (38)$$

which gives a constraint on the AB side of the triangle, corresponding to a circle centered on B, in the $(\bar{\rho}-\bar{\eta})$ plane.

4.4 $B_s^0 - \overline{B}_s^0$ oscillations.

The ratio between the Standard Model expectations for Δm_d and Δm_s is given by the following expression :

$$\frac{\Delta m_d}{\Delta m_s} = \frac{m_{B_d} f_{B_d}^2 B_{B_d} \eta_{B_d} |V_{td}|^2}{m_{B_s} f_{B_s}^2 B_{B_s} \eta_{B_s} |V_{ts}|^2} \quad (39)$$

Neglecting terms of order $O(\lambda^4)$, $|V_{ts}|$ is independent of ρ and η and is equal to $|V_{cb}| \times (1 - \frac{\lambda^2}{2})$. A measurement of the ratio $\frac{\Delta m_d}{\Delta m_s}$ gives the same type of constraint, in the $\bar{\rho}-\bar{\eta}$

plane, as a measurement of Δm_d because it is also proportional to the length of the side AB of the unitarity triangle. This ratio is expected to be less dependent on the absolute values of f_B and B_B , and lattice QCD predicts [36]:

$$\xi = \frac{f_{B_s} \sqrt{B_{B_s}}}{f_{B_d} \sqrt{B_{B_d}}} = 1.17 \pm 0.06 \pm 0.12. \quad (40)$$

The first error corresponds to the present uncertainty of this evaluation inside the quenched approximation and the second error is related to the quenched approximation itself.

The present limit on Δm_s allows to restrict the accessible domain for the $\bar{\rho}$ and $\bar{\eta}$ parameters.

Measurements of Δm_d , $|V_{ub}|$ and $|\epsilon_K|$ can be used also to define the most probable region for Δm_s and $f_{B_d} \sqrt{B_{B_d}}$.

5 Present constraints on the $\bar{\rho}$ and $\bar{\eta}$ parameters.

5.1 The methods

The constraints on $\bar{\rho}$ and $\bar{\eta}$ have been obtained in two ways.

These parameters can be determined by fitting their values from the three expressions given in (23), (25), (38), (39) for, respectively, $\frac{|V_{ub}|}{|V_{cb}|}$, $|\epsilon_K|$, Δm_d , $\frac{\Delta m_d}{\Delta m_s}$ and the corresponding measurements. Extra constraints have been added on A , m_t , B_K , $f_{B_d} \sqrt{B_{B_d}}$, ξ and the QCD parameters entering in the expression of $|\epsilon_K|$, whereas uncertainties on the other parameters have been neglected. The list of parameters used in this analysis is given in Table 2.

An equivalent approach has been developed which consists in building up the two dimensional probability distribution for $\bar{\rho}$ and $\bar{\eta}$. This is done in the following way.

- a point uniformly distributed in the $(\bar{\rho} - \bar{\eta})$ plane, is chosen,
- values for the different parameters entering into the equations of constraints are obtained using random generations extracted from Gaussian distributions
- the predicted values for the four quantities, $\frac{|V_{ub}|}{|V_{cb}|}$, $|\epsilon_K|$, Δm_d and $\frac{\Delta m_d}{\Delta m_s}$ are then obtained and compared with present measurements. A weight is computed assuming that the measurements have Gaussian errors. As an example, the weight corresponding to the constraint provided by the measurement of Δm_d is:

$$w^i(\Delta m_d) \propto \exp -((\Delta m_d(m_{\text{meas.}}) - \Delta m_d(A^i, \rho^i, \eta^i, f_{B_d}^i, B_{B_d}^i, m_t^i, \eta_{B_d}^i))^2 / 2\sigma(\Delta m_d)^2) \quad (41)$$

where $\sigma(\Delta m_d)$ is the measurement error on Δm_d . The final weight is equal to the product of the four weights.

- the sum of all weights, over the $(\bar{\rho} - \bar{\eta})$ plane, is normalized to unity and contours corresponding to 68% and 95% confidence levels have been defined.

today's values	references	"year 2000"	status
$A = 0.81 \pm 0.04$	this paper	± 0.025	varied
$\frac{ V_{ub} }{ V_{cb} } = 0.08 \pm 0.02$	[13]	± 0.01	varied
$\overline{m}_c(m_c) = (1.3 \pm 0.1) \text{ GeV}/c^2$	[13]		varied
$f_K = 0.161 \text{ GeV}/c^2$	[13]		fixed
$\Delta m_K = (0.5333 \pm 0.0027) \times 10^{-2} \text{ ps}^{-1}$	[13]		fixed
$\Delta m_d = (0.469 \pm 0.019) \text{ ps}^{-1}$	[38]	$\pm 0.015 \text{ ps}^{-1}$	varied
$\Delta m_s > 8.0 \text{ ps}^{-1}$ at 95% C.L.	[38]	12.5 ps^{-1} at 95% C.L.	varied
$ \epsilon_K = (2.258 \pm 0.0018) \times 10^{-3}$	[13]		fixed
$\overline{m}_t(m_t) = (168 \pm 6) \text{ GeV}/c^2$	[11]	$\pm 5 \text{ GeV}/c^2$	varied
$B_K = 0.90 \pm 0.09$	this paper	± 0.05	varied
$f_{B_d} \sqrt{B_{B_d}} = (200 \pm 50) \text{ MeV}$	this paper	$\pm 30 \text{ MeV}$	varied
$\frac{f_{B_s} \sqrt{B_{B_s}}}{f_{B_d} \sqrt{B_{B_d}}} = 1.17 \pm 0.13$	this paper	± 0.06	varied
$\eta_1 = 1.38 \pm 0.53$	[27],[28]		varied
$\eta_2 = 0.574 \pm 0.004$	[27],[28]		fixed
$\eta_3 = 0.47 \pm 0.04$	[27],[28]		varied
$\eta_B = 0.55 \pm 0.01$	[27]		fixed
$G_F = (1.16639 \pm 0.00002) \times 10^{-5} \text{ GeV}^{-2}$	[13]		fixed
$m_W = 80.33 \pm 0.15 \text{ GeV}/c^2$	[13]		fixed
$m_{B_d^0} = 5.279 \pm 0.002 \text{ GeV}/c^2$	[13]		fixed
$m_{B_s^0} = 5.375 \pm 0.006 \text{ GeV}/c^2$	[13]		fixed
$m_K = 0.49767 \pm 0.00003 \text{ GeV}/c^2$	[13]		fixed
$\lambda = 0.2205 \pm 0.0018$	[13]		fixed

Table 2: Values of the parameters entering into the expressions for Δm_d (eq. 38), $|\epsilon_K|$ (eq. 25), $\frac{|V_{ub}|}{|V_{cb}|}$ (eq. 23) and $\Delta m_d/\Delta m_s$ (eq. 39). The column , "year 2000", gives the expected uncertainties on the parameters for which an improvement is forseen before that time.

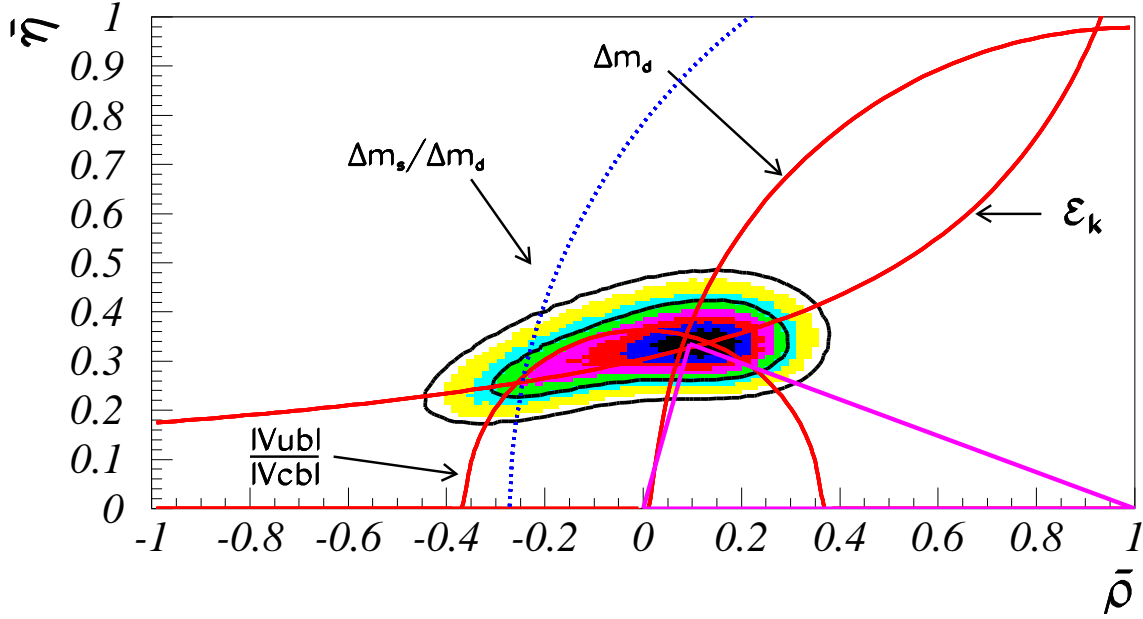


Figure 2: The allowed region for $\bar{\rho}$ and $\bar{\eta}$ using the parameters listed in Table 2. The contours at 68% and 95 % are shown. The continuous lines correspond to the constraints obtained from the measurements of $\frac{|V_{ub}|}{|V_{cb}|}$, $|\epsilon_K|$ and Δm_d . The dotted curve corresponds to the 95 % C.L. upper limit obtained from the experimental limit on Δm_s . This last constraint has not been included when determining the allowed region. The position of the apex of the triangle corresponds to the most probable value which coincides with the fitted value given in (42).

It has been verified that the two approaches give equivalent results by comparing these contours with those given by the fitting procedure. The second approach allows to construct the probability distribution for several parameters of interest such as Δm_s , $\sin 2\alpha$ and $\sin 2\beta$. In this approach non-Gaussian distributions for the errors on the experimental measurements of the constraints and on the parameters entering into the equations of the constraints can be used. An example is given in (Section 5.2.2).

5.2 Results with present measurements.

5.2.1 Measured values of the $\bar{\rho}$ and $\bar{\eta}$ parameters:

The contours corresponding to 68% and 95% confidence levels are shown in Figure 2. The result of the fit gives :

$$\bar{\rho} = 0.10^{+0.13}_{-0.38} ; \quad \bar{\eta} = 0.33^{+0.06}_{-0.09} \quad (42)$$

It has been verified that, when using the same set of values for the parameters listed in Table 2 as those given in [37], the fitted values for $\bar{\rho}$ and $\bar{\eta}$ and their corresponding errors were also similar.

The different sources of error which determine the size of the allowed region are examined in the following. Simplified expressions for the uncertainties on $\bar{\rho}$ and $\bar{\eta}$ have

been obtained assuming that these two parameters are determined by the measurements of Δm_d and $|\epsilon_K|$ respectively. The expressions are:

$$\sigma_{\bar{\rho}} \simeq \frac{\sigma_A}{A} \oplus 0.75 \frac{\sigma_{m_t}}{m_t} \oplus 0.5 \frac{\sigma_{\Delta m_d}}{\Delta m_d} \oplus \frac{\sigma_{f_{B_d}} \sqrt{B_{B_d}}}{f_{B_d} \sqrt{B_{B_d}}} \oplus \sigma_{QCD} \quad (43)$$

$$\frac{\sigma_{\bar{\eta}}}{\bar{\eta}} \simeq 3.3 \frac{\sigma_A}{A} \oplus \frac{\sigma_{m_t}}{m_t} \oplus 0.7 \frac{\sigma_{m_c}}{m_c} \oplus \frac{\sigma_{B_K}}{B_K} \oplus \sigma_{QCD} \quad (44)$$

The last mentioned contribution in these expressions comes from the uncertainty in the evaluation of effects from strong interactions at the next to leading order. Using the central values for the parameters listed in Table 2 and their corresponding uncertainties, the expected error on $\bar{\rho}$ becomes:

$$\sigma_{\bar{\rho}} \simeq 0.050 \oplus 0.027 \oplus 0.020 \oplus 0.25 \oplus 0.01$$

The error on $\bar{\rho}$ is almost entirely due to the uncertainty on $f_{B_d} \sqrt{B_{B_d}}$ which is of theoretical origin (37). Its present value does not allow to profit from the accurate measurement of the Δm_d parameter, which is known at the level of 4% relative error (see Table 2). The possibility of having a more precise determination of f_{B_d} is considered in the section dedicated to the perspectives (Section 6). The second important contribution to the error on $\bar{\rho}$ is coming from the uncertainty on the A parameter extracted from the measurement of $|V_{cb}|$.

For the $\bar{\eta}$ parameter, the corresponding result is obtained:

$$\frac{\sigma_{\bar{\eta}}}{\bar{\eta}} \simeq 0.16 \oplus 0.036 \oplus 0.054 \oplus 0.10 \oplus 0.055$$

The uncertainty on $\bar{\eta}$ is governed by the theoretical uncertainty on B_K and by the measurement error on A . The error on A plays an important role since, for $\rho \simeq 0$, eq. (25) tells that: $|\epsilon_K| \simeq B_K A^4$.

In the considerations, developped in the second part of this paragraph, the effect from the measurement of $\frac{|V_{ub}|}{|V_{cb}|}$, which can further reduce the accessible region, has been neglected.

5.2.2 Measured values for $\bar{\rho}$ and $\bar{\eta}$ when including the current limit on Δm_s .

As mentioned in section 4.4 a possibility to reduce the uncertainty on $\bar{\rho}$ is the measurement of the ratio $\frac{|\Delta m_d|}{|\Delta m_s|}$. The search for $B_s^0 - \bar{B}_s^0$ oscillations has been the object of an intense activity in the last two years. No measurement is available sofar. The best limit comes from the combination of ALEPH, DELPHI and OPAL results [38] :

$$\Delta m_s > 8.0 ps^{-1} \quad \text{at } 95\% C.L. \quad (45)$$

This limit has been obtained in the framework of the amplitude method [39] which consists in measuring, for each value of the frequency Δm_s , an amplitude a and its error $\sigma(a)$. The parameter a is introduced in the time evolution of pure B_s^0 or \bar{B}_s^0 states so that the value $a = 1$ corresponds to a genuine signal for oscillation:

$$\mathcal{P}(B_s^0 \rightarrow (B_s^0, \bar{B}_s^0)) = \frac{1}{2\tau_s} e^{-\frac{t}{\tau_s}} \times (1 \pm a \cos(\Delta m_s t))$$

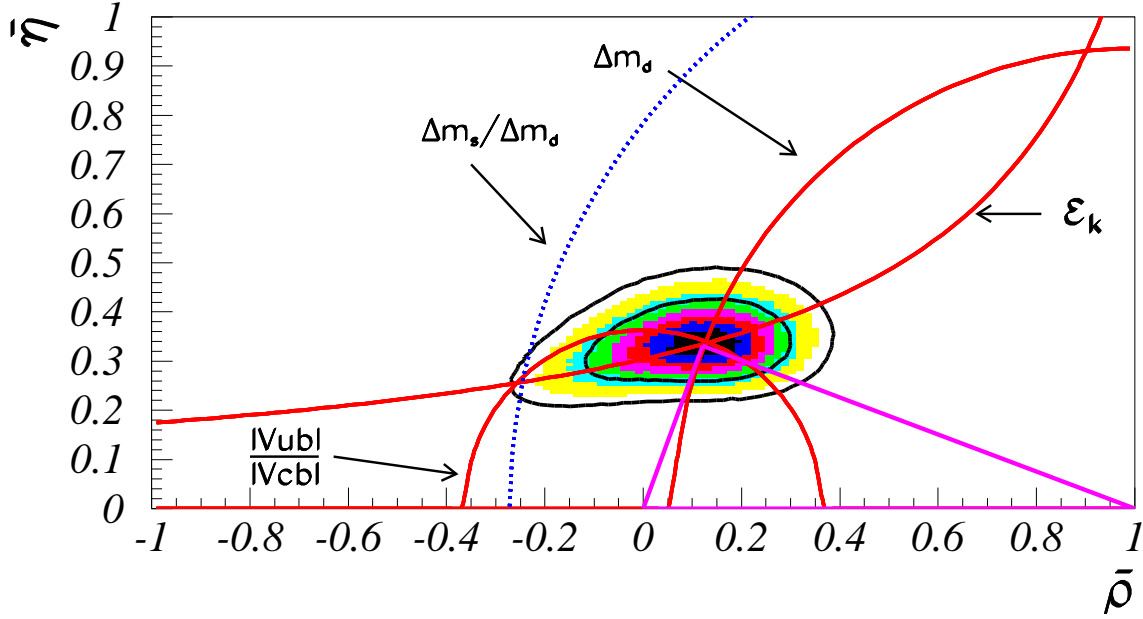


Figure 3: The allowed region for $\bar{\rho}$ and $\bar{\eta}$ using the parameters listed in Table 2. The contours at 68% and 95 % are shown. The full lines correspond to the central values of the constraints given by the measurements of $\frac{|V_{ub}|}{|V_{cb}|}$, $|\epsilon_K|$ and Δm_d . The dotted curve corresponds to the 95 % C.L. upper limit obtained from the experimental limit on Δm_s . This last constraint has been included following the procedure discussed in Section 5.2.2. The ratio ξ has been also varied according to eq. (40).

A randomly distributed decay time distribution which is expected for very large values of Δm_s , corresponds to $a = 0$ and the 95% C.L. excluded region for Δm_s is obtained in evaluating the probability that, in at most 5% of the cases, the observed amplitude is compatible with the value $a = 1$, this corresponds to the condition:

$$a(\Delta m_s) + 1.645\sigma(a(\Delta m_s)) < 1.$$

This limit on Δm_s allows to cut the left side part of the $\bar{\rho} - \bar{\eta}$ region (Figure 3). However the set of measurements $a(\Delta m_s)$ contains more information than the 95% C.L. limit. It is possible to build a χ^2 , which quantifies the compatibility of $a(\Delta m_s)$ with the value $a = 1$, defined as:

$$\chi^2(\Delta m_s) = \frac{(a(\Delta m_s) - 1)^2}{\sigma^2(a(\Delta m_s))}$$

and which can be used as a constraint.

The new allowed region for the $\bar{\rho}$ and $\bar{\eta}$ parameters is shown in Figure 3.

The result of the fit gives :

$$\bar{\rho} = 0.11^{+0.13}_{-0.25} ; \quad \bar{\eta} = 0.33^{+0.06}_{-0.06} \quad (46)$$

It can be noticed that the present limit on Δm_s gives a reduction by a factor of 1.5 on the negative error of $\bar{\rho}$.

A similar fit has been performed using flat distributions for the quantities in which the

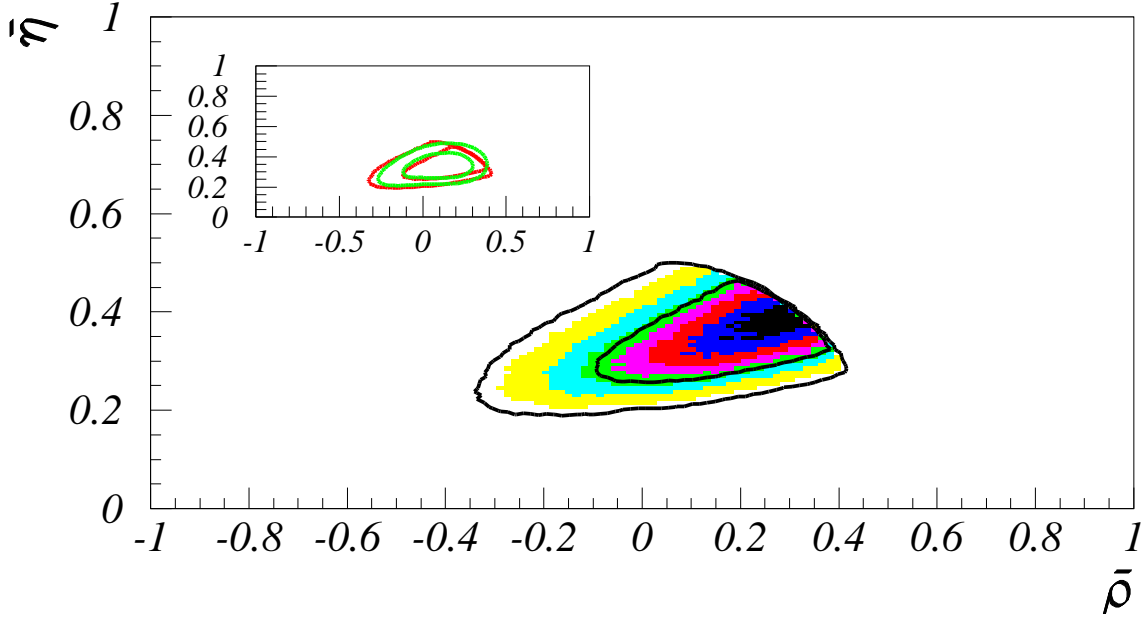


Figure 4: The allowed region for $\bar{\rho}$ and $\bar{\eta}$ using the parameters listed in Table 2. Flat distributions have been used for $\frac{|V_{ub}|}{|V_{cb}|}$, B_K , $f_B\sqrt{B_B}$ and ξ which have the same variance as the previously Gaussian distributions. The contours at 68% and 95 % are shown. The inset shows the comparison between the contours at 68% and 95 % for Gaussian distributions (clearer contours) and for flat distributions (darker countours).

systematic error is dominant. These quantities are $\frac{|V_{ub}|}{|V_{cb}|}$, B_K , $f_B\sqrt{B_B}$ and ξ . The considered variation for these distributions have been chosen such that the new, flat, and the previous, Gaussian, distributions have the same variance. The new allowed region for the $\bar{\rho}$ and $\bar{\eta}$ parameters is shown in Figure 4.

The comparison between the contours at 68% and 95 % of this new allowed region with those obtained with only Gaussian distributions (Figure 3) is shown in the inset of Figure 4. The difference is small and is essentially due to the uncertainty on $\frac{|V_{ub}|}{|V_{cb}|}$.

5.2.3 Simultaneous measurement of $\bar{\rho}$ - $\bar{\eta}$ and $f_{B_d}\sqrt{B_{B_d}}$

Instead of using $f_{B_d}\sqrt{B_{B_d}}$ as an external constraint, this quantity can be also fitted together with the $\bar{\rho}$ and the $\bar{\eta}$ parameters. The result is:

$$\begin{aligned}\bar{\rho} &= 0.12^{+0.15}_{-0.26} ; \quad \bar{\eta} = 0.33^{+0.06}_{-0.07} \\ f_{B_d}\sqrt{B_{B_d}} &= 208^{+30}_{-40} \text{ MeV}\end{aligned}\tag{47}$$

If, in addition, the external constraint on $f_{B_d}\sqrt{B_{B_d}}$ is imposed, the result on the $\bar{\rho}$ and $\bar{\eta}$ parameters is the one given in (46) and $f_{B_d}\sqrt{B_{B_d}} = 205^{+26}_{-35} \text{ MeV}$. This result implies that the constraint coming from the measurement of Δm_d will bring information only if the uncertainty on $f_{B_d}\sqrt{B_{B_d}}$ can be reduced to 30 MeV or below.

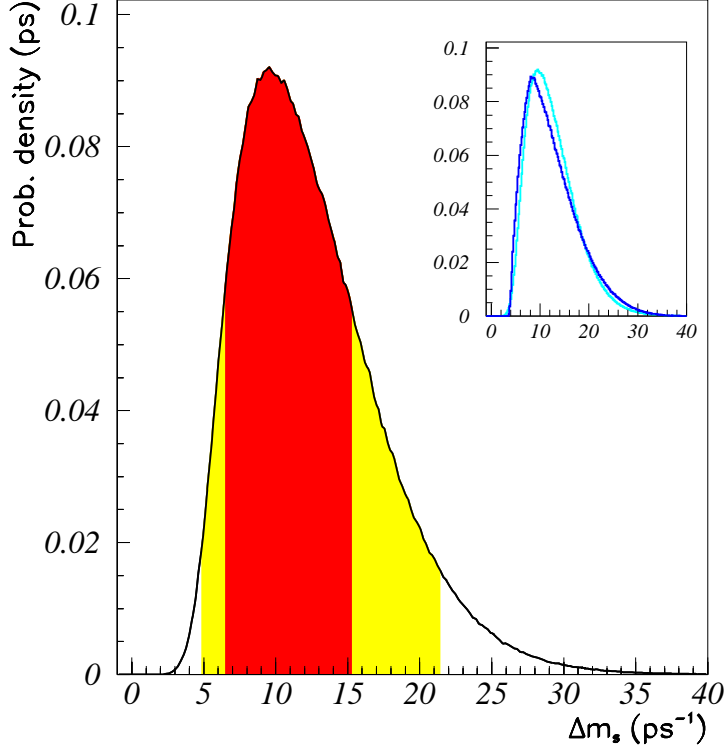


Figure 5: The Δm_s probability distribution obtained with the same constraints as in Figure 2. The dark-shaded and the clear-shaded intervals correspond to 68% and 95 % confidence level regions respectively. The inset shows the comparison between the Δm_s probability distributions for Gaussian distributions (clearer contours) and for flat distributions (darker contours)

5.2.4 Δm_s probability distribution.

One of the advantage of having explicitly built up the two-dimensional probability distribution for $\bar{\rho}$ and $\bar{\eta}$ is that the weights previously defined can be used to obtain the probability distribution for Δm_s . This distribution is shown in Figure 5. It is expected that the value of Δm_s is in the range between 6.5 and 15 ps^{-1} at 68% C.L. The most probable value is around 10 ps^{-1} . At 95 % C.L. Δm_s has to be smaller than 21 ps^{-1} . The current LEP combined lower limit at 8 ps^{-1} is just exploring the one sigma expected region for Δm_s . The Δm_s distribution has been also obtained using flat distributions for the quantities in which the systematic error is dominant as explained at the end of Sec. 5.2.2. At 68% C.L., Δm_s is expected between 5 and 15 ps^{-1} , the most probable value is around 9 ps^{-1} and at 95 % C.L. Δm_s has to be smaller than 22 ps^{-1} . The comparison between the new Δm_s distribution with those obtained with only Gaussian distributions is shown in the inset of Figure 5.

5.2.5 Measured values for $\sin 2\alpha$ and $\sin 2\beta$.

Present measurements of Δm_d , $|V_{ub}|$, $|\epsilon_K|$ and the limit on Δm_s can be used also to define the allowed region in the plane $(\sin 2\alpha, \sin 2\beta)$, where α and β are respectively

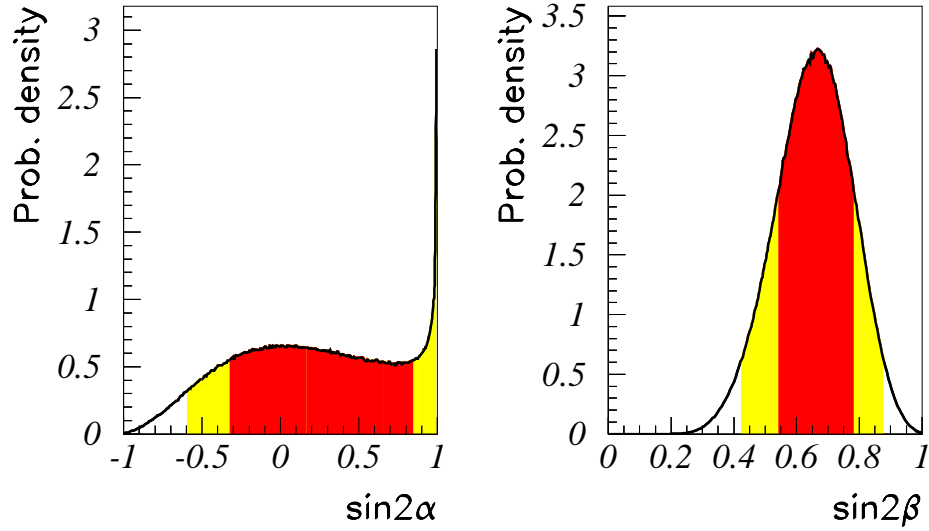


Figure 6: The $\sin 2\alpha$ and $\sin 2\beta$ distributions are shown in the left and right plots respectively. They have been obtained using the same constraints as in Figure 2. The dark-shaded and the clear-shaded intervals correspond to 68% and 95 % confidence level regions respectively.

equal to the angles \widehat{CAB} and \widehat{ABC} of the unitarity triangle. The values of $\sin 2\alpha$ and $\sin 2\beta$ are expected to be measured at future B-factories from the studies of the decays $B_d^0 \rightarrow \pi^+\pi^-$ and $B_d^0 \rightarrow J/\Psi K_s^0$, respectively. With present measurements the following values have been obtained (Figure 6):

$$\sin 2\alpha > -0.60 \text{ at } 95\% C.L., \quad \sin 2\beta = 0.67^{+0.12}_{-0.13} \quad (48)$$

The accuracy on $\sin 2\beta$ is already at the level expected in the year 2000 at B-factories. The value of $\sin 2\alpha$ is more uncertain because it depends a lot on the measurement of $\bar{\rho}$; for the fitted values of $\bar{\rho}$ and $\bar{\eta}$, the error on $\sigma(\sin 2\alpha)$ is typically $\simeq 5 \sigma(\bar{\rho})$. Using flat distributions for the quantities in which the systematic error is dominant, as explained in Sec. 5.2.2, the new value for $\sin 2\beta$ is equal to $0.82^{+0.05}_{-0.22}$.

6 The perspectives

6.1 Improvements on the determination of non-perturbative QCD parameters

6.1.1 The f_B parameter

It has been shown in section 5.2.3 that the accuracy on the measurement of $\bar{\rho}$ can be improved if $f_{B_d}\sqrt{B_{B_d}}$ can be obtained with an uncertainty smaller than 30 MeV.

Direct measurement of f_B . A priori, f_B can be measured using the decay $B^+ \rightarrow \tau^+\nu_\tau$ which proceeds through the annihilation of the \bar{b} and u quarks. The corresponding branching fraction for this process is proportional to the product $f_B^2 \times |V_{ub}|^2$. Thus, following

this procedure, f_B is not directly measured. Furthermore the Standard Model predicts a branching fraction of the order of 7×10^{-5} which is very small as compared to possible sources of background. Present limits from LEP and CLEO experiments are at the level of 5×10^{-4} [40] and 2.2×10^{-3} at 90% C.L. [41] respectively. From the analysis point of view LEP is the most favourable place to perform this measurement but the statistics are too low. At CLEO and future B-factories this measurement seems to be very difficult and a 10% precision seems to be unrealistic.

f_B from lattice QCD calculations: the use of f_{D_s} to evaluate f_B . The study of the decay $D_s^+ \rightarrow \tau^+ \nu_\tau$ or $D_s^+ \rightarrow \mu^+ \nu_\mu$ has two clear advantages with respect to the $B^+ \rightarrow \tau^+ \nu_\tau$ channel. The branching fraction is of the order of 5 %, for the first channel, and f_{D_s} can be directly obtained, since the value of the CKM element $|V_{cs}|$ is well known. From the present measurements of $D_s^+ \rightarrow \tau^+ \nu_\tau$ and $D_s^+ \rightarrow \mu^+ \nu_\mu$ decays, f_{D_s} is derived to be [42] :

$$f_{D_s} = 255 \pm 20 \pm 31 \text{ MeV} \quad (49)$$

The method proposed in the following, to evaluate f_B , consists in using this measurement and the extrapolation from the D to the B sector, as predicted by lattice QCD [43]. At present, the ratio f_{D_s}/f_{D^+} has also to be taken from the theory and the value given in [44] has been used:

$$\frac{f_{D_s}}{f_{D^+}} = 1.10 \pm 0.05 \pm 0.10$$

where the last error is an estimate of uncertainties from the quenching approximation. The ratio f_B/f_D is then obtained using the expected variation, from lattice QCD, of $f \times \sqrt{M}$ as a function of $1/M$ and requiring that the prediction coincides with the measured decay constant in the D region. From the dispersion of present predictions, it has been assumed that this extrapolation gives an additional 10% relative error. It results that:

$$f_{B_d} = 178 \pm 26(\text{exp.}) \pm 18\left(\frac{f_{D_s}}{f_{D^+}}\right) \pm 18\left(\frac{f_B}{f_{D^+}}\right) \text{ MeV} \quad (50)$$

The value obtained for f_{B_d} , in this approach is well compatible with the absolute prediction from lattice QCD (eq. 33) and also with the value favoured by the measurements of $|\epsilon_K|$, Δm_d , $\frac{|V_{ub}|}{|V_{cb}|}$ and the limit on Δm_s , corresponding to eq. (47)

$$f_{B_d} = 178^{+26}_{-34} \text{ MeV} \quad (51)$$

This approach seems promising because accurate experimental measurements can be obtained in future. In the coming years, improvements are expected from CLEO and from LEP on the absolute decay rate $D_s^+ \rightarrow \tau^+ \nu_\tau$ ($D_s^+ \rightarrow \mu^+ \nu_\mu$). A spectacular improvement is expected from a future Tau-Charm factory where f_{D_s} and f_{D^+} can be measured with a relative accuracy of 1.5%. These two measurements can provide very strict constraints on results from lattice QCD. In particular they can validate unquenched evaluations when going from bound states made with an heavy quark and a strange or a non-strange anti-quark. On the other hands a theoretical effort has to be done to further reduce the error from the extrapolation between the D and B mass regions.

6.1.2 B_{B_d} and B_K parameters.

The bag parameters B_K and B_{B_d} cannot be measured experimentally. As it has been shown in Sections 4.2, 4.3 the precision on these parameters is limited by the error related to the quenched approximation. New and more precise results expected in the next future and a better control of the quenched approximation should allow to reach a precision of 5 % on B_K and B_{B_d} .

6.2 Improvements on the determination of the Δm_s frequency

The best limit on Δm_s ($\Delta m_s > 8.0 \text{ ps}^{-1}$ at 95% C.L.) is coming from the combination of the latest analyses from ALEPH, DELPHI and OPAL collaborations at LEP. Improvements are expected by adding new analyses, from the refinement of present ones and from new results from the SLD experiment. From a study, done in DELPHI, the final LEP sensitivity ¹ for Δm_s will be around 12.5 ps^{-1} [45] which is above the expected most probable value of 10 ps^{-1} as shown in Figure 5. It has been also demonstrated [45] that this result is mainly limited by the available statistics collected by the experiments. A gain of a factor four in statistics would allow to have a sensitivity up to $\Delta m_s = 16 \text{ ps}^{-1}$. In this case, for a value of $\Delta m_s = 10 \text{ ps}^{-1}$, which corresponds to the most probable value, at present, a measurement, with a precision better than 15 % could also be performed [45].

6.3 Improvements on A , m_t and $\frac{|V_{ub}|}{|V_{cb}|}$

As shown in Section 3 the measurement of $|V_{cb}|$ comes from the average of two methods. The first one uses the values of the inclusive lifetime and of the inclusive semileptonic branching fraction of B hadrons. Its precision is limited by the accuracy on the theoretical parameter γ_c . An improvement on its determination is expected [20],[46]. The second method uses the measurement of $Br(B \rightarrow D^* \ell \nu)$ in the framework of HQET. The precision of this measurement is limited by experimental errors. On statistical errors, improvements are expected mainly from the CLEO experiment. The main systematic uncertainties come from the errors on the B_d^0 lifetime, on the B_d^0 production rate in jets and on the D^{**} production rate in B hadron semileptonic decays. These parameters can be more precisely measured at LEP in the near future. All these improvements could allow to reach a precision of ± 0.001 on $|V_{cb}|$ which corresponds to an uncertainty of ± 0.025 on A .

Theoretical improvements are also expected to extract the ratio $\frac{|V_{ub}|}{|V_{cb}|}$ [46]. A possible error of ± 0.01 will be considered in the perspectives.

In addition the final analyses of CDF and D0 at Fermilab should allow to reach a precision of $\pm 5 \text{ GeV}$ on the top mass.

¹ In the amplitude approach described in Section 5.2.2, it is possible to compute the exclusion probability \mathcal{P}_{limit} of being able to set a limit for a given value of Δm_s , with the studied channel. The sensitivity is the value of Δm_s corresponding to $\mathcal{P}_{limit} = 0.5$.

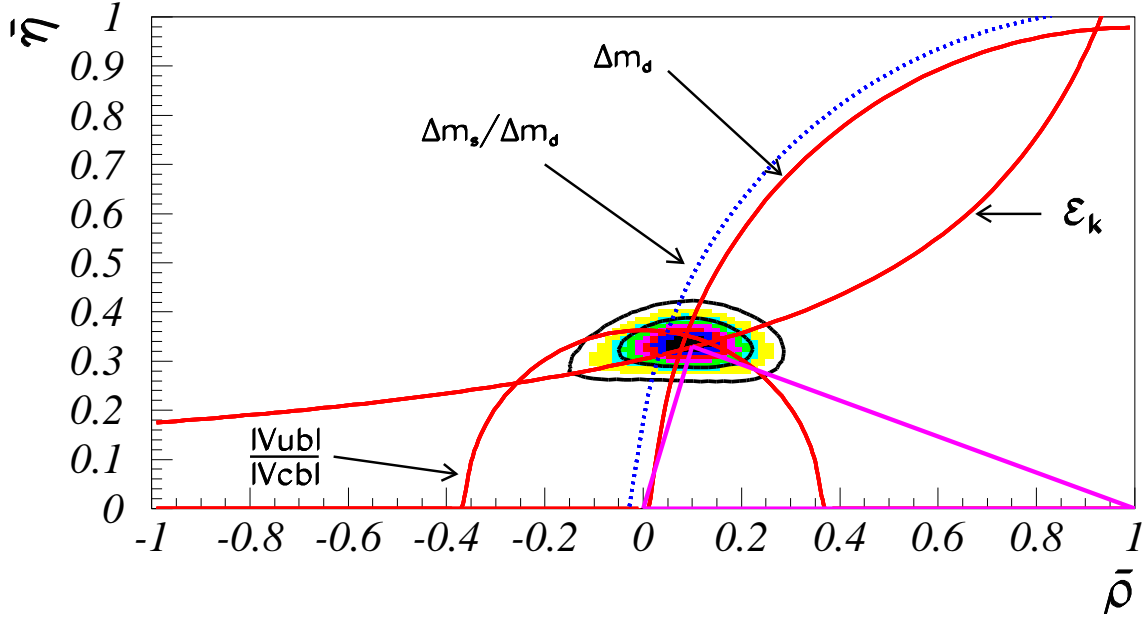


Figure 7: The $\bar{\rho}$ - $\bar{\eta}$ allowed region in the “Year 2000” scenario. Contours at 68% and 95 % are indicated.

6.4 Different scenari.

Three scenari are presented in this section. It has to be noticed that the central values obtained in each case for $\bar{\rho}$, $\sin 2\alpha$ or f_B are rather arbitrary because the informations on these quantities are obtained with the present central values and reduced uncertainties on the different parameters entering into the measurements. Only quoted uncertainties on these quantities are meaningful.

6.4.1 “Year 2000” scenario.

The central values and uncertainties of the parameters, used for this scenario, are given in the third column of Table 2. This scenario, named “Year 2000”, corresponds to the possible situation at the threshold of the year 2000, before the start up of B-factories. It includes the “possible” latest CLEO and LEP results. A sensitivity at 12.5 ps^{-1} on Δm_s is considered and, in addition, better estimates for the f_B , B_B , ξ and B_K parameters on which uncertainties have been reduced by a factor of about two. The error used for f_B comes from the current determination of f_{D_s} whereas the central value is kept the same as in eq. (33). The improvements on A , m_t and $\frac{|V_{ub}|}{|V_{cb}|}$, described in previous paragraphs, have been included. The results are:

$$\bar{\rho} = 0.09^{+0.07}_{-0.11} ; \quad \bar{\eta} = 0.335^{+0.034}_{-0.033} \quad (52)$$

The new allowed region for the $\bar{\rho}$ and $\bar{\eta}$ parameters is shown in Figure 7. It corresponds to:

$$\sin 2\alpha = 0.24 \pm 0.41; \quad \sin 2\beta = 0.65^{+0.06}_{-0.07} \quad (53)$$

The $\sin 2\alpha$, $\sin 2\beta$ distributions are shown in Figure 8.

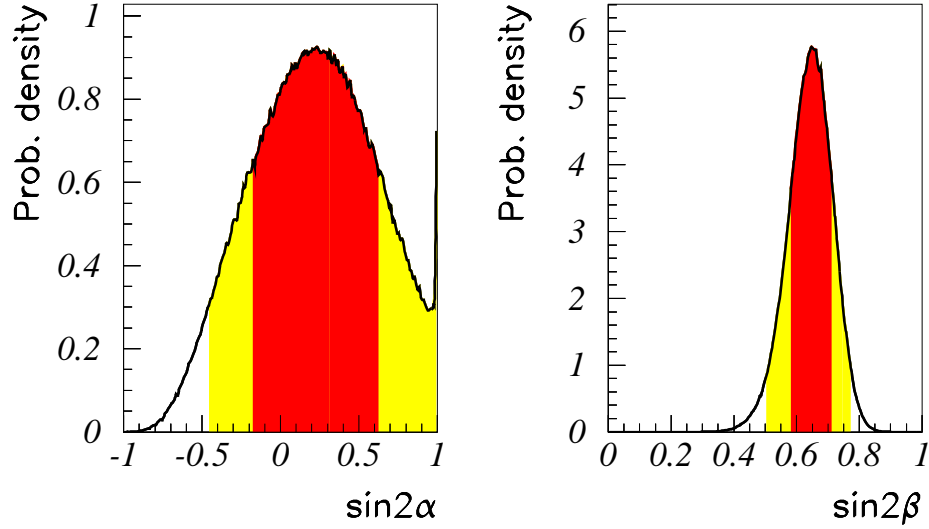


Figure 8: The $\sin 2\alpha$ and $\sin 2\beta$ distributions, shown in the left and right plots respectively, have been obtained using the constraints corresponding to the values of the parameters expected in the “Year 2000” scenario. The dark-shaded and the clear-shaded intervals correspond to 68% and 95 % confidence level regions respectively.

Two scenarios are presented in the following. The “ τ -Charm” scenario which considers the possibility of having a τ -Charm factory operating at the beginning of the next millenium, allowing an accurate control of non-perturbative QCD parametrs. The CP-phases scenario which shows the importance of the direct measurement of $\sin 2\alpha$ and $\sin 2\beta$. Several experimental facilities have been approved for the latter purpose whereas none τ -charm factory is foreseen yet. The aim of separately showing the two scenarios is to stress their complementary and to underline, at least once, the importance of having a τ -Charm factory project soon operating.

6.4.2 “ τ -Charm” scenario.

This scenario considers the possibility of having a τ -Charm factory operating at the beginning of the next millenium.

In the previous scenario it has been shown that the $\bar{\rho}$ parameter is still known three times less precisely than the $\bar{\eta}$ parameter. This is mainly due to the uncertainty on f_B . At a τ -Charm factory f_{D_s} and f_{D^+} can be measured with a precision at the per cent level. Following the approach described in 6.1.1, f_B may be determined with a precision better than 5%. To reach this goal a joint effort, between experimentalists and theorists working on lattice QCD, is needed.

Assuming 2.5 % accuracy on the quantity $f_{B_d}\sqrt{B_{B_d}}$ ($f_{B_d}\sqrt{B_{B_d}} = 200 \pm 5 \text{ MeV}$), the expected accuracy on the $\bar{\rho}$ and $\bar{\eta}$ parameters comes out to be:

$$\bar{\rho} = 0.080 \pm 0.048 \quad ; \quad \bar{\eta} = 0.334 \pm 0.034 \quad (54)$$

and the new allowed region is shown in Figure 9. The information coming from Δm_s result is not used, the reason being that the measurement of $f_{B_d}\sqrt{B_{B_d}}$ and of $\frac{\Delta m_d}{\Delta m_s}$ give

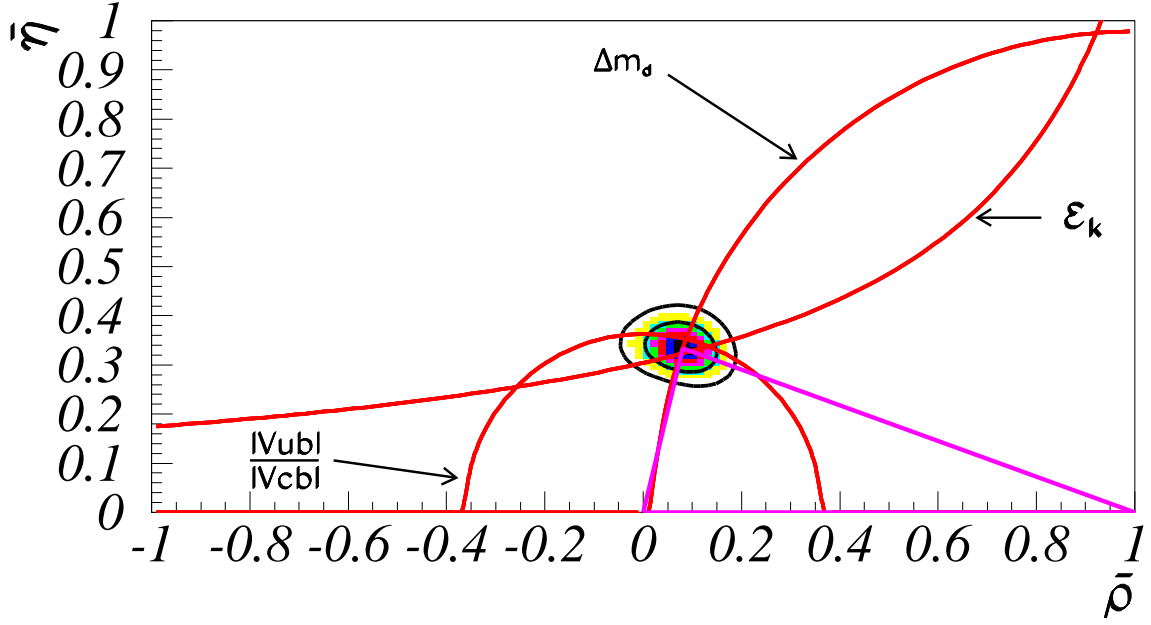


Figure 9: The $\bar{\rho}$ - $\bar{\eta}$ allowed region in the “ τ -Charm” scenario. Contours at 68% and 95 % C.L. are indicated.

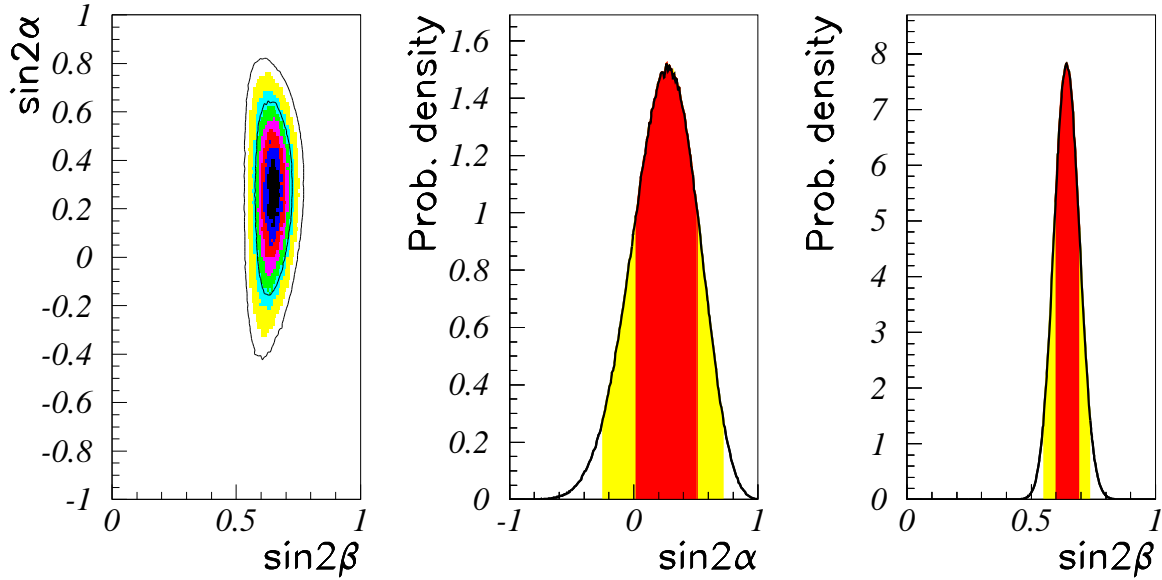


Figure 10: The $\sin 2\alpha$ and $\sin 2\beta$ distributions have been obtained using the constraints corresponding to the values of the parameters expected in the “ τ -Charm” scenario. The dark-shaded and the clear-shaded intervals correspond, respectively, to 68% and 95 % confidence level regions.

Scenarii	$\bar{\rho}$	$\bar{\eta}$	Δm_s (ps^{-1})	$f_B \sqrt{B_B} (\text{MeV})$
At-present	$0.10^{+0.13}_{-0.38}$	$0.33^{+0.06}_{-0.09}$	$10^{+5.0}_{-3.5}$	-
At-present + Δm_s	$0.11^{+0.13}_{-0.25}$	0.33 ± 0.06	$[> 8 \text{ ps}^{-1} \text{ at } 95\% \text{C.L.}]$	208^{+30}_{-40}
Year-2000	$0.09^{+0.07}_{-0.11}$	$0.335^{+0.034}_{-0.035}$	$[\text{sensitivity at } 12.5 \text{ ps}^{-1}]$	± 15
τ -Charm	0.080 ± 0.048	0.335 ± 0.034	$12.8 \pm 1.8 \text{ ps}^{-1}$	$[\pm 5]$
CP-phases	$0.121^{+0.029}_{-0.026}$	0.331 ± 0.026	$[\text{sensitivity at } 12.5 \text{ ps}^{-1}]$	± 9

Table 3: Results on $\bar{\rho}$ - $\bar{\eta}$, Δm_s and $f_{B_d} \sqrt{B_{B_d}}$ in the different scenarii. Apart from the present measurements, the central values of these quantities -with the exception of the one for $\bar{\eta}$ - are not meaningful, only expected errors have to be retained. The results on Δm_s and on $f_B \sqrt{B_B}$ are given in squared brackets when they correspond to values given as constraints and which are not improved at the end of the fitting procedure.

the same type of constraint. In practice the constraint at ± 5 MeV on $f_{B_d} \sqrt{B_{B_d}}$ has the same effect as a measurement of $\Delta m_s = 12.8 \pm 1.8 \text{ ps}^{-1}$.

The corresponding values for $\sin 2\alpha$ and $\sin 2\beta$ are:

$$\sin 2\alpha = 0.23 \pm 0.25; \quad \sin 2\beta = 0.65 \pm 0.04, \quad (55)$$

and their expected distributions are shown in Figure 10.

The inclusion of the Δm_s constraint slightly improves the errors on the $\bar{\rho}$ and $\bar{\eta}$ parameters.

6.4.3 “CP-phases” scenario.

In this scenario, the direct measurement of $\sin 2\alpha$ and $\sin 2\beta$ is considered.

Several experiments have been approved for this purpose. HERA-B at DESY and the Fermilab experiments (the upgrades of D0 and CDF experiments) are mainly sensitive to $\sin 2\beta$ via the reconstruction of the decay $B \rightarrow J/\psi K_s^0$. As shown in Section 5.2.5 the current precision on $\sin 2\beta$, obtained from indirect measurements in the framework of the Standard Model and of the C.K.M. matrix, is ± 0.13 and it is expected to improve down to ± 0.07 in the year 2000. The HERA-B experiment foresees to have a precision on $\sin 2\beta$ of the order of ± 0.20 and an accuracy of ± 0.10 is expected at Fermilab experiments.

The e^+e^- asymmetric B-factories (BaBar at SLAC and BELLE at KEK) can measure both $\sin 2\beta$ and $\sin 2\alpha$, the latter via the reconstruction of the decay $B \rightarrow \pi^+ \pi^-$.

Assuming that these two quantities are measured with a precision of:

$$\delta(\sin 2\beta) = \pm 0.10 \quad ; \quad \delta(\sin 2\alpha) = \pm 0.10$$

and considering that the other parameters, listed in Table 2, are known with an accuracy corresponding to the “Year-2000” scenario, the expected precisions on $\bar{\rho}$ and $\bar{\eta}$ are then:

$$\bar{\rho} = 0.121^{+0.029}_{-0.026} \quad ; \quad \bar{\eta} = 0.331 \pm 0.026 \quad (56)$$

This corresponds to an equivalent precision of $\pm 9 \text{ MeV}$ on the f_{B_d} parameter.

The new $\bar{\rho}$ - $\bar{\eta}$ allowed region is shown in Figure 11. It should be reminded that B-factories will contribute to reduce the $\bar{\rho} - \bar{\eta}$ region by performing also additional measurements on

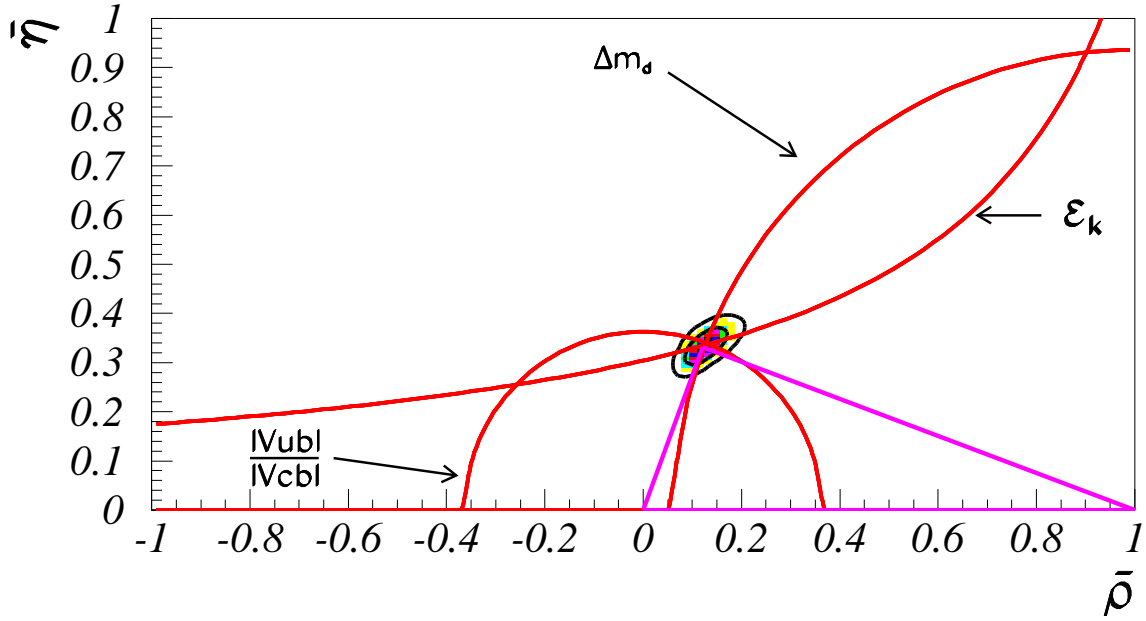


Figure 11: The $\bar{\rho}$ - $\bar{\eta}$ allowed region in the “CP-phases” scenario. Contours at 68% and 95 % C.L. are indicated.

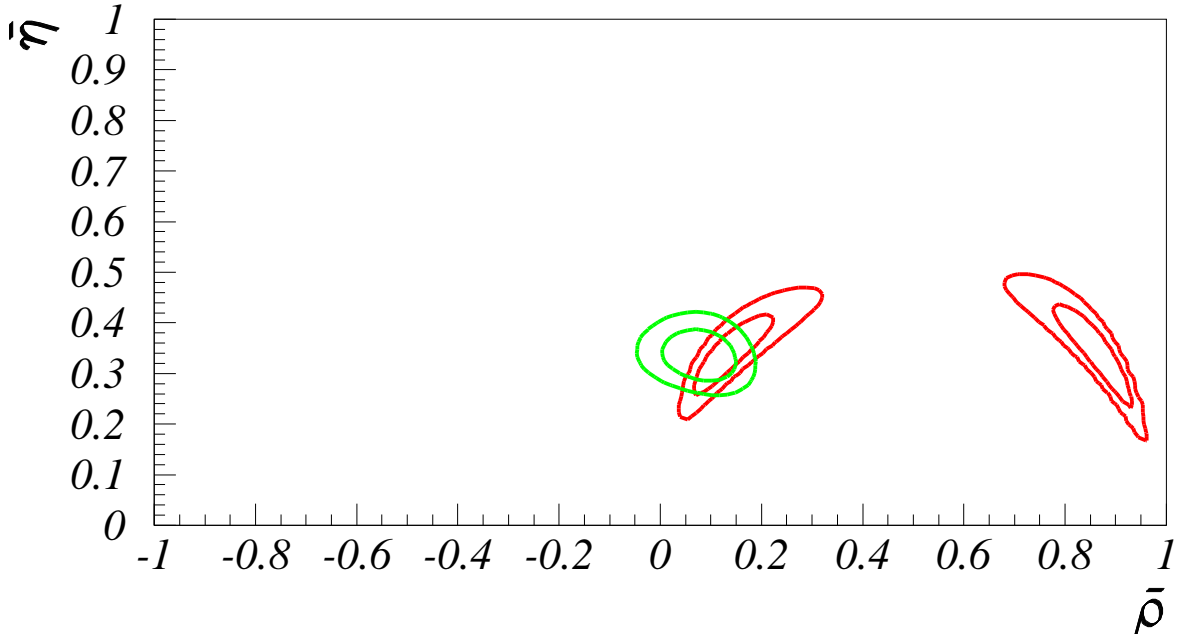


Figure 12: The contours at 68% and 95 % C.L. in the $\bar{\rho}$ - $\bar{\eta}$ plane obtained in the “ τ -Charm” scenario (clearer contours) are compared with those coming from the measurement of the quantities $\sin 2\alpha$ and $\sin 2\beta$, alone, with ± 0.10 accuracy at future B -factories (darker contours).

Scenarii	$\sin 2\alpha$	$\sin 2\beta$
At-present	> -0.60 at 95% C.L	$0.67^{+0.12}_{-0.13}$
Year-2000	0.24 ± 0.41	$0.65^{+0.06}_{-0.07}$
τ -Charm	0.23 ± 0.25	0.65 ± 0.04
CP-phases	$[\pm 0.10]$	$[\pm 0.10]$

Table 4: Results for $\sin 2\alpha$ and $\sin 2\beta$ in the different scenarii. For the CP-phases scenario the errors refer to the direct measurement of the angles.

$\frac{|V_{ub}|}{|V_{cb}|}$ and on $|V_{cb}|$.

It will be of interest to compare the $\bar{\rho}$ - $\bar{\eta}$ allowed regions in the two following different approaches :

- the precise measurements of the sides of the unitary triangle, which requires an accurate control of non-perturbative QCD parameters (“Year-2000” and “ τ -Charm” scenarii) corresponding to a determination of f_{B_d} with an error of 10 MeV or better,
- the precise measurements of the angles (“CP-phases” scenario).

The two selected $\bar{\rho}$ - $\bar{\eta}$ allowed regions are shown in Figure 12.

A summary of the results expected on $\bar{\rho}$ - $\bar{\eta}$, Δm_s and $f_{B_d}\sqrt{B_{B_d}}$ in the different scenarii is given in Table 3. Table 4 gives the summary for the $\sin 2\alpha$ and $\sin 2\beta$ variables.

7 Possible effects from supersymmetric particles.

In this section are discussed the additional contributions to Δm_d and to $|\epsilon_K|$ expected to come from the presence of new physics beyond the Standard Model. The effect of new physics can be parametrized by introducing an extra parameter Δ . This formulation is valid in any extension of the Standard Model in which the flavour changes are controlled by the V_{CKM} matrix.

In case, for instance, of Δm_d the expression (30) becomes

$$\Delta m_d = \frac{g^4}{192m_W^2\pi^2} |V_{tb}|^2 |V_{td}|^2 m_{B_d} f_{B_d}^2 B_{B_d} \eta_B \Delta \quad (57)$$

The same quantity Δ appears in the expression of $|\epsilon_K|$.

The Δ parameter can be written

$$\Delta = x_t(F(x_t) + \Delta_{NewPhysics}) \quad (58)$$

The Standard Model predicts : $\Delta = 2.55 \pm 0.15$, where the error takes into account the uncertainty on the top mass. The present data can be then fitted using the new expressions for Δm_d and $|\epsilon_K|$ fitting Δ together with the parameters $\bar{\rho}$ and $\bar{\eta}$, the result is :

$$\begin{aligned} \bar{\rho} &= 0.20^{+0.19}_{-0.38} \quad ; \quad \bar{\eta} = 0.29^{+0.13}_{-0.15} \\ \Delta &= 3.2^{+5.9}_{-1.9} \end{aligned} \quad (59)$$

Scenarii	Δ	m_{SUSY} , $\tan \beta = 1$	$\tan \beta=1.5$	$\tan \beta = 5$
At-present	$3.2^{+5.9}_{-1.9}$	> 55	no limit	no limit
Year-2000	± 1.0	> 120	> 85	> 60
τ -Charm	± 0.7	> 140	> 105	> 75
CP-phases	± 0.6	> 150	> 115	> 80

Table 5: *Results on the Δ parameter in the different scenarii. The limits on m_{SUSY} are given in GeV/c^2 at 95 % C.L.*

The same fit has been performed for the scenarii presented in the previous section and results have been summarized in Table 5. Since the central values of all parameters entering into the fit have been fixed at the presently measured ones, only the expected error on Δ is given.

To see the possible implications of such a precision on the Δ parameter a particular example is discussed in the following, in the framework of the MSSM extension of the Standard Model, stressing the constraints that can be obtained essentially on the masses of the lightest supersymmetric particles. The theoretical framework is discussed in [47]. In this framework light stop-right (\tilde{t}) and higgsinos are considered assuming that $\tan^2\beta$ is lower than m_t/m_b and that the stop-left and the gauginos are heavy. In this scenario Δ can be written :

$$\Delta_{NewPhysics} = (\Delta_H + \Delta_{SUSY}) \quad (60)$$

Δ_H and Δ_{SUSY} denote the contributions to the box diagram from charged Higgs boson and from R-odd supersymmetric particles respectively; for the latter, contributions of the stop-right (\tilde{t}) and of the charged higgsino ($\tilde{\chi}$) are considered. The expression for these quantities are given in [47]. In the region of masses between 60 and 150 GeV/c^2 , Δ_{SUSY} dominates over Δ_H because the former depends on $(m_{\tilde{t}} + m_{\tilde{\chi}})/2$ and is enhanced by the presence of the factor (m_t^2/m_{SUSY}^2) and, due to the term $1/\sin^4(\beta)$, is rapidly growing for $\tan\beta \simeq 1$.

In the following the term Δ_H has been neglected and the stop-right and the charged higgsino are supposed to have the same mass (generically indicated as m_{SUSY} in the following). The quantity Δ is then defined as:

$$\Delta = x_t(F(x_t) + \Delta_{SUSY}(x_{t_{\tilde{\chi}}}, x_{\tilde{\chi}}, \beta)) \quad (61)$$

where $x_t = (m_t^2/m_W^2)$, $x_{t_{\tilde{\chi}}} = (m_t^2/m_{\tilde{\chi}}^2)$ and $x_{\tilde{\chi}} = (m_{\tilde{t}}^2/m_{\tilde{\chi}}^2)$. Its variation is shown in Figure 13, as a function of the higgsino (stop-right) mass. It can be noticed that Δm_d can be large for small values of this mass and values of $\tan\beta$ close to unity.

The present result (59) does not give any stringent constraint on SUSY parameters. Sofar no limit on the mass of the lightest supersymmetric particle can be set. This can be clearly seen in Figure 14. The same fit has been repeted for the scenarii presented in the previous section and results have been summarized in Table 5. A limit on m_{SUSY} is obtained, using as a central value for Δ , the Standard Model expectation. Significant limits can be set for small values of $\tan\beta$.

It is important to stress that also in the SUSY framework the V_{CKM} matrix is unitary.

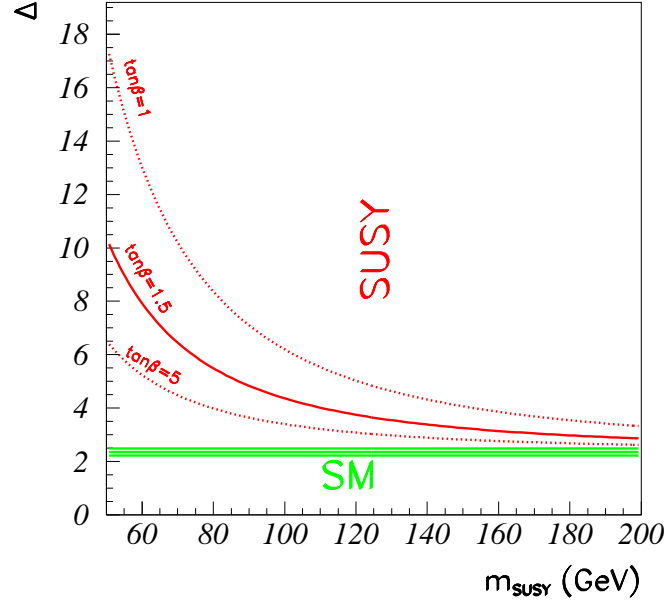


Figure 13: The curves represent Δ as a function of m_{SUSY} for different values of $\tan\beta$. The horizontal lines correspond to the value of Δ expected in the Standard Model with the uncertainty due to the top mass.

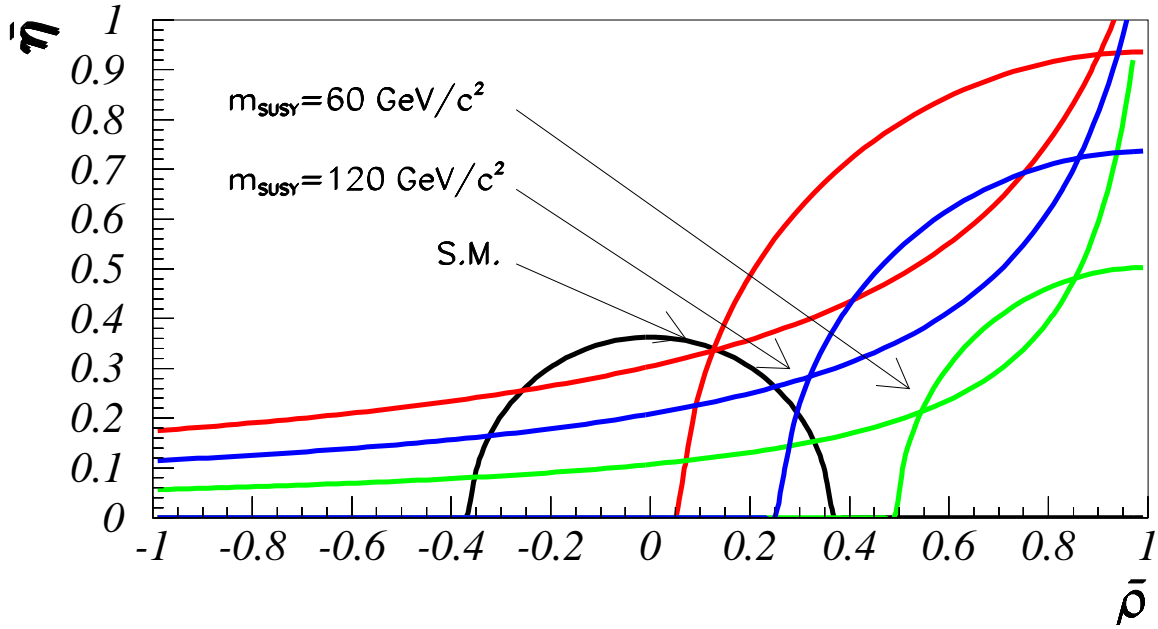


Figure 14: The compatibility of the constraints on Δm_d , $|\epsilon_K|$ and $\frac{|V_{ub}|}{|V_{cb}|}$ is shown in three different scenarii. The constraint on $\frac{|V_{ub}|}{|V_{cb}|}$ does not change while from left to right the constraints on Δm_d and $|\epsilon_K|$ change from the Standard Model scenario to two SUSY scenarii with $m_{\text{SUSY}} = 120 \text{ GeV}/c^2$ and $60 \text{ GeV}/c^2$ and $\tan\beta = 1.5$.

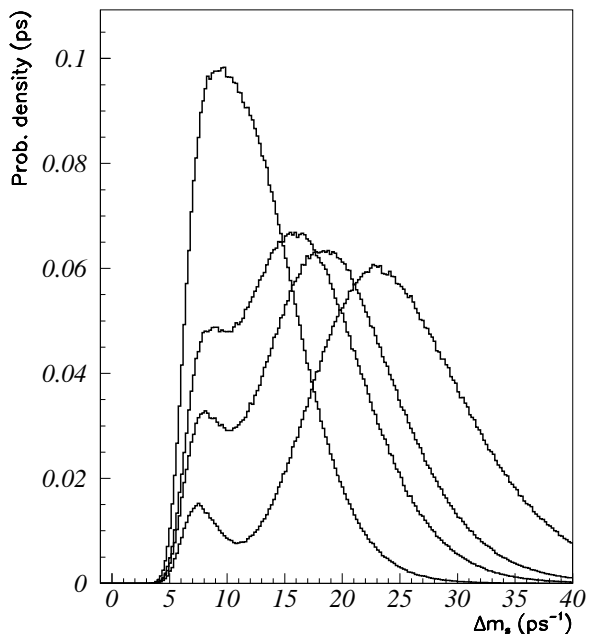


Figure 15: Δm_s probability distributions obtained with the same constraints as in Figure 2. The first distribution, on the left, corresponds to the Δm_s probability distribution as obtained in the Standard Model (same as in Figure 5). The other distributions are obtained in the supersymmetric scenario using $\tan\beta = 1.5$ and, from left to right, $m_{SUSY} = 160, 120$ and $80 \text{ GeV}/c^2$.

It can happen that the different constraints, as they are expressed in the Standard Model parametrization, do not converge at the same point. SUSY can then be invoked. Finally it is important to stress that, in this approach, the ratio $\Delta m_d/\Delta m_s$ remains the same as in the Standard Model in terms of $\bar{\rho}$ and $\bar{\eta}$. But as, in this scenario, the favoured values for $\bar{\rho}$ and $\bar{\eta}$ are not the same as in the Standard Model (see Figure 14), the value of Δm_s will be different. This effect is shown in Figure 15. The Δm_s probability distribution moves towards higher values for decreasing values of the mass of the lightest supersymmetric particle.

8 Conclusions.

The Wolfenstein parametrization describes the V_{CKM} matrix in terms of four parameters : λ , A , ρ , η and λ is known with a precision better than 1%.

The recent theoretical progress and the new precise measurements of the inclusive lifetime and of the semileptonic branching fraction of B hadrons, as well as a new approach in the HQET framework which makes use of the measurement of $BR(B \rightarrow D^* \ell \nu)$, allow to get a precise value of A : $A = 0.81 \pm 0.04$.

The $\bar{\rho}$ and $\bar{\eta}$ parameters have been determined using the constraints from the measurements of $\frac{|V_{ub}|}{|V_{cb}|}$, $|\epsilon_K|$ and Δm_d and the limit on Δm_s . The $\bar{\eta}$ parameter which is related to the CP violating phase is different from zero and is equal to $\bar{\eta} = 0.35 \pm 0.06$. A further reduction on the uncertainty on A will allow to decrease the uncertainty on $\bar{\eta}$. The $\bar{\rho}$

parameter is at present poorly known. Its determination has been recently improved by the limit obtained on Δm_s , the fitted value is $\bar{\rho} = 0.10^{+0.14}_{-0.21}$. The uncertainty on $\bar{\rho}$ is dominated by the precision on the non-perturbative QCD parameter $f_B\sqrt{B_B}$. It has been shown, that using available constraints from $\frac{|V_{ub}|}{|V_{cb}|}$, $|\epsilon_K|$, Δm_d and Δm_s , this quantity is equal to: $f_{B_d}\sqrt{B_{B_d}} = 208^{+30}_{-40} MeV$. This measurement, which is obtained assuming the validity of the Standard Model, improves the theoretical determination of this quantity, $f_{B_d}\sqrt{B_{B_d}} = 200 \pm 50 MeV$. This shows that a better determination of $\bar{\rho}$ can be obtained if $f_{B_d}\sqrt{B_{B_d}}$ is measured with a precision better than $\pm 30 MeV$.

It has been also shown that the value of Δm_s cannot be too large in the Standard Model (Figure 15). It is expected to lie, within one sigma, in the range between 6.5 and 15 ps^{-1} , the most probable value being 10 ps^{-1} . With the present combined lower limit of $\Delta m_s > 8.0 ps^{-1}$ at 95 % C.L. LEP experiments are then exploring a very interesting region. It has been also shown that the introduction of light supersymmetric particles in the loops can significantly displace the Δm_s distribution towards higher values.

A significant comparison between a future direct measurement of $\sin 2\beta$ and the present evaluation of this quantity, $\sin 2\beta = 0.67^{+0.12}_{-0.13}$, in the framework of the Standard Model has been also presented. If no progress is obtained in the evaluation of f_B , the evaluation of $\sin 2\alpha$ from the measurement of the sides of the unitary triangle will remain too uncertain to be compared with the direct measurement.

A precise determination of f_{D_s} and f_{D^+} at a future τ -Charm factory can be used to verify lattice QCD evaluations of these quantities. A precise determination of f_B can then be obtained using these measurements and the extrapolation from the D to the B sector, as predicted by lattice QCD. A restricted region can be isolated in the $(\bar{\rho}-\bar{\eta})$ plane which has a similar extension as expected from direct measurement of $\sin 2\alpha$ and $\sin 2\beta$ with ± 0.1 uncertainty.

Finally the present data have been analyzed in a SUSY model, in the framework of a given scenario. So far no stringent limits can be set on the mass of the lightest supersymmetric particles. The Standard Model fails if the different measurements are not compatible with the same values of $\bar{\rho}$ and $\bar{\eta}$. It has been shown that in the SUSY framework different parametrizations of $|\epsilon_K|$ and Δm_d are obtained providing the extra terms to accomodate this eventual problem.

Acknowledgements

We would like to thank C.W. Bernard for the useful interactions on the subjects related to non perturbative QCD parameters and F. Zwirner for clarifications on the theoretical aspects of the paper. We profit all along this work from the support of F. Richard and D. Treille and we benefit from stimulating discussions with them. They are warmly thanked. A special thanks to W. Venus for the useful observations and for the careful reading of the document. Finally thanks to the DELPHI Collaboration in which we are working and without which this work could not have been done.

References

- [1] A. D. Sakharov, *ZhETF Pis. Red.* **5** (1967) 32.
A. D. Sakharov, *JETP Lett.* **4** (1967) 24.
- [2] P. Huet and E. Sather, *Phys. Rev.* **D53** (1996) 4578.
M. B. Gavela, P. Hernandez, J. Orloff and O. Pene, CERN-TH-94/7368.
- [3] B.J. Bjorken and S.L. Glashow, *Phys. Lett.* **11** (1994) 255.
Y. Hara, *Phys. Rev.* **B701** (1964) 134.
Z. Maki and Y. Ohnuki, *Prog. Theor. Phys.* **32** (1964) 144.
- [4] N. Cabibbo, *Phys. Rev. Lett.* **10** (1963) 351.
- [5] S.L. Glashow, J. Iliopoulos and L. Maiani, *Phys. Rev.* **D2** (1970) 1285.
- [6] J.J. Aubert et al., BNL Spectrometer Coll., *Phys. Rev. Lett.* **33** (1974) 1404.
J.E. Augustin et al., SPEAR Coll., *Phys. Rev. Lett.* **33** (1974) 1406.
- [7] V. Luth et al., SPEAR Coll., *Phys. Rev. Lett.* **34** (1975) 1125.
G. Goldhaber et al., SPEAR Coll., *Phys. Rev. Lett.* **37** (1976) 255.
I. Peruzzi et al., SPEAR Coll., *Phys. Rev. Lett.* **37** (1976) 569.
- [8] M. L. Perl et al., MARK I Coll., *Phys. Rev. Lett.* **35** (1975) 1489.
M. L. Perl et al., MARK I Coll., *Phys. Lett.* **63B** (1976) 466.
- [9] S.W. Herb et al., Fermilab P.C. Coll., *Phys. Rev. Lett.* **39** (1977) 252.
W. R. Innes et al., Fermilab P.C. Coll., *Phys. Rev. Lett.* **39** (1977) 1240.
- [10] C. Albjär et al., UA1 Coll., *Phys. Lett.* **B186** (1987) 247.
H. Albrecht et al., ARGUS Coll., *Phys. Lett.* **B192** (1987) 245.
A. Bean et al., CLEO Coll., *Phys. Rev. Lett.* **58** (1987) 183.
- [11] F. Abe et al., CDF Coll., *Phys. Rev. Lett.* **74** (1995) 2626.
S. Abachi et al., D0 Coll., *Phys. Rev. Lett.* **74** (1995) 2632.
Average by P. Tipton, Plenary Session, ICHEP 96 (25-31 July 1996, Warsaw).
- [12] M. Kobayashi and T. Maskawa, *Prog. Theor. Phys.* **49** (1973) 652.
- [13] R.M. Barnett et al. Particle Data Group (PDG) , Review of Particle Properties, *Phys. Rev.* **D54** (1996) 1.
- [14] L. Wolfenstein, *Phys. Rev. Lett.* **51** (1983) 1945.
- [15] G. Altarelli, N. Cabibbo, G. Corbo, L. Maiani and G. Martinelli, *Nucl. Phys.* **B208** (1982) 365.
M. Shifman, N.G. Uraltsev and A. Vainshtein, *Phys. Rev.* **D51** (1995) 2217.
M. Luke and M.J. Savage, *Phys. Lett.* **B321** (1994) 88.
P. Ball, M. Beneke and V.M. Braun , CERN-TH/95-65,UM-TH-95-07,hep-ph/9503492.
M. Neubert CERN-PPE/96-55.

- [16] I. Bigi, B. Blok, M. Shifman, N.G. Uraltsev and A.I Vainhestein , in " B Decays" edited by S. Stone , World Scientific (1994) 132 .
I. Bigi et al., *Phys. Lett.* **B323** (1994) 408.
I. Bigi UND-HEP-95-BIG01.
M. Neubert, *Phys. Lett.* **B338** (1994) 84.
P. Ball and U. Nierste, *Phys. Rev.* **D50** (1994) 5841.
- [17] T. E. Browder and K. Honscheid UH 511-816-95, OHSTPY-HEP-E95-010 (1995).
- [18] J.D. Richman and P.R.Burchat UCSB-HEP-95-08, Stanford-HEP-95-01 (1995).
- [19] A. Stocchi LAL 96-38 (May 1996).
- [20] I. Bigi, M. Shifman and N.G. Uraltsev, " Aspects of Heavy Quark Theory", hep-ph/9703290
- [21] B Lifetimes LEP Working Group, Averages for Winter Conferences (March 1997)
<http://wwwcn.cern.ch/~claires/lepblife.html>
- [22] LEP-ElectroWorking Group CERN-PPE/96-183.
- [23] I. Caprini and M.Neubert, *Phys. Lett.* **B380** (1996) 376.
A. Czarnecki, *Phys. ReV. Lett.* **76** (1996) 4124.
M. Neubert, *Phys. Lett.* **B338** (1994) 84.
T. Mannel, *Phys. ReV* **D50** (1994) 428.
M. Shifman, N.G. Uraltsev and A. Vainshtein, *Phys. Rev.* **D51** (1995) 2217.
- [24] H. Albrecht et al., ARGUS Coll., *Zeit. Phys.* **C57** (1993) 533.
B. Barish et al., CLEO Coll., *Phys. ReV.* **D51** (1995) 1014.
B. Buskulic et al., ALEPH Coll., CERN-PPE/96-150.
P. Abreu et al., DELPHI Coll., *Zeit. Phys.* **C71** (1996) 531.
K. Ackerstaff et al., OPAL Coll., CERN-PPE/96-162.
- [25] A.J. Buras, M.E. Lautenbacher and G. Ostermaier, *Phys. ReV.* **D50** (1994) 3433.
A.J.Buras , MPI-Pht/95-17 (1995).
- [26] G. Buchalla, A.J. Buras and M.E. Lautenbacher MPI-PH/95-104, to appear in ReV. of Mod. Phys.
- [27] G. Buchalla, A.J. Buras and M.K. Harlander, *Nucl. Phys.* **B337** (1990) 313.
W.A. Kaufman, H. Steger and Y.P. Yao, *Mod. Phys. Lett.* **A3** (1989) 1479.
J. M. Flynn, *Mod. Phys. Lett.* **A5** (1990) 877.
A. Datta, J. Frölich and E.A. Paschos, *Z. Phys.* **C46** (1990) 63.
S. Herrlich and U. Nierste, *Nucl. Phys.* **B419** (1994) 292.
A.J. Buras MPI-PHT/95-88,TUM-T31-97/95 (1995).
- [28] A.J. Buras, M. Jasmin and P.H. Weisz, *Nucl. Phys.* **B347** (1990) 491.
- [29] C.W. Bernard private communication.
- [30] P. Paganini PHD Thesis, LAL 96-18 (May 1996), in french.

- [31] C.T. Sachrajda in "B decays" 2nd Edition edited by S. Stone W.S. (1994) 602.
A. Soni, *Nucl. Phys.* **B47** (1996) 43. A.J.Buras MPI-Pht/95-17 (1995).
- [32] A. Duncan et al. FERMILAB-PUB-94/164-T.
C.W. Bernard, J.N. Labrenz and A. Soni, *Phys. ReV.* **D49** (1994) 2536.
T. Draper and C. Mc Neile, *Nucl. Phys.* **B34** (1994) 453.
- [33] E. Bagan et al., *Phys. Lett.* **B278** (1992) 457.
M. Neubert, *Phys. ReV.* **D45** (1992) 2451.
- [34] S. Capstick and S. Godfrey, *Phys. ReV.* **D41** (1990) 2856.
- [35] P. Colangelo, G. Nardulli, M. Pietroni, *Phys. ReV.* **D43** (1991) 3002.
- [36] A. Abada et al., *Nucl. Phys.* **B376** (1992) 172.
- [37] A. Ali and D. London, DESY 96-140, UdeM-GPP-TH-96-38 (july 1996).
- [38] B Oscillation LEP Working Group
Averages for Hawaii (24-27 March 1997) and Moriond QCD (22-29 March 1997)
Conferences <http://www.cern.ch/LEPBOSC>.
- [39] H.G. Moser and A. Roussarie, *Nucl. Instr. and Meth.* **A384** (1997) 491.
- [40] D. Buskulic et al., ALEPH Coll., *Phys. Lett.* **B343** (1994) 444.
(L3 Coll.) L3 note 1988 - Contributed paper to the Warsaw conf.
- [41] J.P. Alexander et al., CLEO Coll., CLEO-CONF 94-5 submitted to *Phys. ReV. Lett.*
- [42] S. Aoki et al., (WA75 Collaboration), *Prog. Theor. Phys.* **89** (1993) 131.
J. P. Alexander et al., CLEO Collaboration, CLEO-CONF 95-22.
J. Z. Bai et al., BES Collaboration, *Phys. Rev. Lett.* **74** (1995) 4599.
K. Kodama et al., E653 Collaboration, *Phys. Lett.* **B382** (1996) 299.
L3 Collaboration, CERN-PPE/96-198 (1996) submitted to *Phys. Lett. B*.
Average by J. Richmann, Plenary Session, ICHEP 96 (25-31 July 1996, Warsaw).
- [43] C.W Bernard, J.N. Labrenz and A. Soni, *Phys ReV.* **D49** (1994) 2536.
- [44] C. Alexandrou, S. Gusken, F. Jegerlehner, K. Schilling and R. Sommer, *Phys. Lett.* **B256** (1991) 60.
C. Alexandrou, S. Gusken, F. Jegerlehner, K. Schilling and R. Sommer, *Zeit. Phys.* **C62** (1994) 659.
R.M. Baxter et al., UKQCD Coll., *Phys. ReV* **D49** (1994) 1594.
K.M. Bitar et al., *Phys. ReV* **D49** (1994) 3546.
C. Bernard, T. Draper, G. Hockney and A. Soni, *Phys. ReV.* **D38** (1998) 3540.
M.B. Gavela et al., *Nucl. Phys.* **B306** (1988) 677.
M.B. Gavela et al., *Phys. Lett.* **B206** (1988) 113.
T.A. Grand and D.R. Loft, *Phys. ReV.* **D38** (1988) 954.
A. Abada et al., *Nucl. Phys.* **B376** (1992) 172.
C. Bernard, J. Labrenz and A. Soni, *Phys. ReV.* **D49** (1994) 2536.

- H. Hamber, *Phys. Rev.* **D39** (1989) 896.
- T. Bhattacharya and R. Gupta (for LANL-Coll.) Proceeding of international conference on lattice field theories "Lattice 94", to be published in *Nucl. Phys.* **B** (Proc. Suppl.).
- [45] M. Canepa et al., DELPHI-Internal Note DELPHI 97-10 PHYS 669.
- [46] I. Bigi and T. Mannel symposium for the 60th Birthday of K. Zalewski to appear in Acta Physica Polonica.
- [47] A. Brignole, F. Feruglio and F. Zwirner, *Zeit. Phys.* **C71** (1996) 679.